CP violation effects and high energy neutrinos

Paolo Lipari*
Dipartimento di Fisica, Università di Roma "La Sapienza" and INFN, Sezione di Roma, P. A. Moro 2, I-00185 Roma, Italy
(Received 5 February 2001; published 29 June 2001)

This work discusses critically the prospects of measuring CP and T violation effects in high-energy neutrino factories. For this purpose we develop, in the standard framework with three neutrino flavors, simple expressions for the oscillation probabilities in matter that are valid for high E_ν. All CP violating effects vanish $\propto E_\nu^{-3}$ and are very difficult to detect with high-energy neutrinos. A significantly easier task is the determination of the absolute value $|\delta|$ of the phase in the ν mixing matrix that controls the CP and T violation effects, performing precision measurements of the CP and T conserving part of the oscillation probabilities.

DOI: 10.1103/PhysRevD.64.033002 PACS number(s): 14.60.Pq, 11.30.Cp, 12.15.Ff

I. INTRODUCTION

Measurements of atmospheric [1] and solar [2] neutrinos have recently given evidence or strong indications that neutrino oscillations exist. These results, together with important constraints from reactor experiments [3], give us precious information about the neutrino masses and mixing that we hope will be of great value to develop an understanding of physics beyond the standard model. In this work we will assume that the oscillations are only between the three known ν flavors, and the surprising and potentially extraordinarily important results of the Liquid Scintillation Neutrino Detector (LSND) [4] will be neglected.

There is currently a very active interest in the planning of future experimental studies on ν flavor transitions; the possibility to observe CP and T violation effects in ν oscillations (see Refs. [5–7]) is perhaps the most fascinating perspective. Neutrino factories [8] have been proposed as a method to provide intense and well controlled beams to perform these studies. Two fundamental properties of a neutrino factory experiment are the energy E_μ of the muon beam and the neutrino path length L. Many proponents of a neutrino factory experimental program are advocating high E_μ [9], in fact as high as technically possible ($E_\mu \sim 50$ GeV or more) and a long path length ($L \sim 3000$–7000 km). Other proponents [10–12] are advocating a much lower muon energy ($E_\mu \sim 1$ GeV) and a shorter path length ($L \sim 100$ km) (for the possibility of a low-energy ν factory, see Ref. [13]). A critical discussion of the limits and merits of the two options is necessary.

The study of direct T-violation effects, comparing, for example, the probabilities for the transitions $\nu_\mu \to \nu_e$ and $\nu_e \to \nu_\mu$, is in principle very attractive [14]; however, until ν beams of extraordinary purity become technically feasible, this study requires the identification of the flavor and electric charge of $e^\pm$; this is very difficult to do in a very massive detector such as those required for these studies.

The study of CP violation effects suffers because of a fundamental problem: it is essentially impossible to construct on Earth two CP antisymmetric long baseline experiments, because ν's or $\overline{\nu}$'s propagate in a medium of electrons and quarks (and not positrons and antiquarks). The effects of the medium on the ν flavors transitions are in general large, and even in the presence of a CP symmetric fundamental Lagrangian one will find $P(\nu_\alpha \to \nu_\beta) \neq P(\nu_\beta \to \nu_\alpha)$.

The fundamental motivation of the "low-energy option" is to perform the measurements where the asymmetry induced by the matter effects is neglibly small. Since the matter effects grow with E_ν, this requires low-energy neutrinos; however, because of the difficulty in focusing low-energy neutrinos, the smallness of interaction cross sections, and the difficulty of flavor identifications the experimental challenges are daunting.

The key point in favor of the choice of a very high E_μ for a neutrino factory is that the rate of neutrino events increases $\propto E_\mu^3$. This impressively rapid growth of the event rate is readily understood as the consequence of two effects: the average energy of the secondary neutrinos grows linearly with E_μ, and to a good approximation $\sigma_\nu \propto E_\nu$; moreover, the angular opening of the neutrino beam shrinks as $\gamma^{-2} = (E_\mu / m_\mu)^{-2}$, correspondingly, the intensity of the ν fluence at a far detector increases as $\propto E_\mu^2$. What is not often sufficiently stressed is that increasing E_μ one has to pay a very high price: the fluence of lower energy neutrinos (for a constant number of muon decays) is suppressed $\propto E_\mu^{-1}$. For example, assuming a perfect focusing, nonpolarized muon beam, and approximating $\beta_\mu \simeq 1$, the fluence of electron (anti)neutrinos is

$$\phi_{\nu_e}(E_\nu) = \frac{12 N_\mu}{\pi L^2} \frac{E_\nu^2}{m_\mu^2 E_\mu} \left(1 - \frac{E_\nu}{E_\mu}\right) \Theta[E_\mu - E_\nu], \qquad (1)$$

where N_μ is the number of useful muon decays, m_μ is the muon mass, and Θ is the step function (the fluence vanishes for $E_\nu > E_\mu$). Examples of the fluence are shown in Figs. 1 and 2. The key point is the fact that for E_ν much smaller than E_μ the fluence has the simple form $\propto E_\nu^2 / E_\mu$.

What is important in the experimental program of course is not the number of ν events but the size of the effects of the oscillations on the event rates, and actually still more important is the size of the *new* effects that one wants to study. The oscillation probabilities are suppressed for high E_ν, and

*Also at Research Center for Cosmic Neutrinos, ICRR, University of Tokyo, Japan.

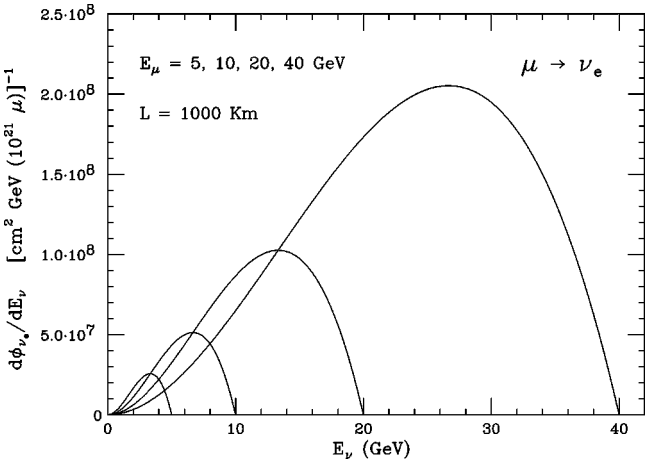

FIG. 1. Electron neutrino fluence ($d\phi_{\nu_e}/dE_\nu$) in a neutrino factory machine. The different curves are calculated for a fixed number of unpolarized μ decays, with different energy: $E_\mu = 5$, 10, 20, and 40 GeV. Note that increasing E_μ the integrated ν fluence increases $\propto E_\nu^2$, but the fluence at low energy decreases.

therefore it is not immediately obvious that the rapid growth of the event rate with increasing E_μ is sufficient to compensate for the suppression of the oscillation probability for higher energy neutrinos. One should also take into account the fact that larger E_ν means larger matter effects, and therefore requires a larger ''subtraction'' to extract the fundamental CP violation effects from the data.

The purpose of this paper is to analyze the size of the CP violation effects for high-energy neutrinos. In this work ''high energy'' means the energy range where, for a given ν path length L, the transition probabilities decrease monotonically to zero with growing E_ν. This happens for

$$E_\nu \gtrsim \frac{|\Delta m^2_{23}|L}{2\pi} = 0.81 \left(\frac{L}{10^3 \text{ km}} \right) \left(\frac{|\Delta m^2_{23}|}{3\times 10^{-3} \text{ eV}^2} \right) \text{ GeV}, \tag{2}$$

that is, for E_ν larger than few GeV even for the longest possible distances. This is the energy range where the proposed high-energy neutrino factories will have most of their rate.

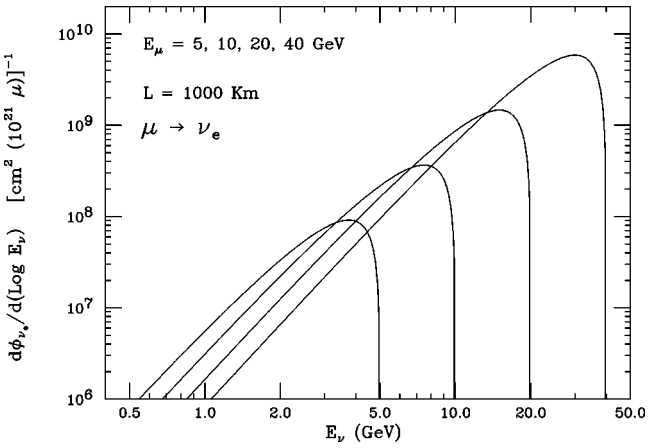

FIG. 2. Electron neutrino fluence in a neutrino factory machine ($d\phi_{\nu_e}/d \log E_\nu$).

As we will discuss in more detail later [see Eq. (32)], for large E_ν the oscillation probabilities have the following dominant functional dependences on the ν energy and the path length:

$$\begin{aligned} P_{\nu_e\rightarrow\nu_\mu} &\sim E_\nu^{-2} L^2, \\ \Delta P_{\nu_e\rightarrow\nu_\mu}(CP) &\sim E_\nu^{-3} L^3, \\ \Delta P_{\nu_e\rightarrow\nu_\mu}(\text{matter}) &\sim E_\nu^{-3} L^4. \end{aligned} \tag{3}$$

The key point is that the CP violation effects vanish rapidly with increasing energy. Also important to note is the fact that the fundamental CP violation effects and matter effects have the same asymptotic energy dependence, but different dependences on the path length L. Integrating these probabilities over the expected energy spectrum for a neutrino factory far detector one finds the following scaling laws for different signals:

$$\begin{aligned} \text{Rate} &\sim E_\mu^3 L^{-2}, \\ \text{Rate}_{\nu_e\rightarrow\nu_\mu} &\sim E_\mu L^0, \\ \Delta\text{Rate}_{\nu_e\rightarrow\nu_\mu}(CP) &\sim E_\mu^0 L, \\ \Delta\text{Rate}_{\nu_e\rightarrow\nu_\mu}(\text{matter}) &\sim E_\mu^0 L^2. \end{aligned} \tag{4}$$

The rate of ''oscillated events'' is approximately independent from the path length L and grows linearly with E_μ. The first effect is the result of cancellation between the decrease $\propto L^{-2}$ of the neutrino fluence, and the growth $\propto L^2$ of the oscillation probabilities with increasing distance. The E_μ dependence is the result of the combination of the decrease of the oscillation probability $\propto E_\nu^{-2}$, with the growth of the neutrino fluence and cross section. The contribution of CP (or T) violation effects on the event rate is, however, approximately independent of E_μ reflecting a cancellation of of the energy depedence $\Delta P_\nu(CP) \propto E_\nu^{-3}$ with the growth of the neutrino fluence and cross section. The CP and T violation effects are therefore more and more difficult to observe with increasing E_μ, because the size of the CP violating effects on the rate is constant, while the ''background'' due to the CP conserving part of the oscillation probability increases linearly with E_μ.

The simple argument that we have outlined is apparently in conflict with the results of previous works that claim [15,16] that the larger the E_μ the higher the sensitivity to the phase δ. The reason for this apparent discrepancy is simple to understand and quite instructive. The leading term of the oscillation probability

$$P_{\text{leading}} = P^{(0)}_{\nu_\mu\rightarrow\nu_e} = P^{(0)}_{\nu_e\rightarrow\nu_\mu} = P^{(0)}_{\nu_\mu\rightarrow\bar{\nu}_e} = P^{(0)}_{\nu_e\rightarrow\bar{\nu}_\mu} = A_{\text{lead}} \frac{L^2}{E_\nu^2} \tag{5}$$

is equal for all four channels related by a *CP* or *T* operation; however, the constant $A_{\rm lead}$ depends on the value of $\cos\delta$. The rate of oscillated events generated by this term is independent from L and grows linearly with E_μ; therefore, in principle, the higher the muon energy the more precisely the constant $A_{\rm lead}$ can be measured, and $\cos\delta$ determined. A significant part of the sensitivity (or ''reach'' in parameter space) for the phase δ claimed for high-energy neutrino factories actually can be understood simply as the result of a very high precision measurement of the leading term in the oscillation probability.

There are two important considerations that should, however, be made. The first one is that to transform a measurement of the constant $A_{\rm lead}$ into a measurement of $\cos\delta$ requires independent measurements with sufficient precision also of all other parameters in the neutrino mass matrix (two squared mass differences and three angles) and a sufficiently precise knowledge of the material along the neutrino path. A second consideration is that this measurement has a fundamental ambiguity. All *CP* violating effects are proportional to $\sin\delta$. The leading term in the oscillation probability is a *CP* and *T* invariant quantity, and in fact depends only on the module $|\sin\delta|$. A measurement of $\cos\delta$ that resulted in a value different from 0 or 1 would imply the existence of *CP* and *T* violations effects in the lepton sector and allow a prediction of their size but not of their sign. Of course, such a result would be of extraordinary importance, however, its limitations should be clearly understood.

The paper is organized as follows: in the next section we discuss our conventions for the neutrino mixing matrix, Sec. III gives a qualitative discussion of the ''geometrical meaning'' of the phase δ, Sec. IV discusses the ν mixing in matter, and Secs. V and VI discuss the ν oscillation probabilities in vacuum and in a homogeneous medium. In these sections we develop an expression for the oscillation probability in matter as a power series in E_ν^{-1} that can be very useful for an understanding of the potential of high-energy machines. Sections VII and VIII contain a discussion and some conclusions. Appendix A contains a detailed derivation of the most important result of this paper [Eq. (32)]; additional material is in Apppendixes B and C.

II. THE NEUTRINO MIXING MATRIX

We will consider in this work oscillations among three neutrinos. The flavor and mass eigenstates are related by a unitary mixing matrix U:

$$|\nu_\alpha\rangle=\sum_j U_{\alpha j}|\nu_j\rangle. \tag{6}$$

For $\overline{\nu}$'s the mixing is given by the complex conjugate matrix U^*. The mixing matrix U can be parametrized in terms of three mixing angles (θ_{12}, θ_{13}, θ_{23}) and one *CP* violating phase δ. We will use the convention suggested by the Particle Data Group (PDG) [17]:

$$\begin{aligned} U&=\begin{pmatrix}1&0&0\\0&c_{23}&s_{23}\\0&-s_{23}&c_{23}\end{pmatrix}\begin{pmatrix}c_{13}&0&s_{13}e^{-i\delta}\\0&1&0\\-s_{13}e^{i\delta}&0&c_{13}\end{pmatrix}\begin{pmatrix}c_{12}&s_{12}&0\\-s_{12}&c_{12}&0\\0&0&1\end{pmatrix}\\ &=\begin{pmatrix}c_{12}c_{13}&s_{12}c_{13}&s_{13}e^{-i\delta}\\-s_{12}c_{23}-c_{12}s_{13}s_{23}e^{i\delta}&c_{12}c_{23}-s_{12}s_{13}s_{23}e^{i\delta}&c_{13}s_{23}\\s_{12}s_{23}-c_{12}s_{13}c_{23}e^{i\delta}&-c_{12}s_{23}-s_{12}s_{13}c_{23}e^{i\delta}&c_{13}c_{23}\end{pmatrix}, \end{aligned} \tag{7}$$

where we have used the notation $s_{jk}=\sin\theta_{jk}$ and $c_{jk}=\cos\theta_{jk}$. We need to specify a convention for the labeling of the mass eigenstates. We will define the state $|\nu_3\rangle$ as the ''most isolated'' neutrino and $|\nu_1\rangle$ as the lightest between the remaining two states. Calling m_1, m_2, and m_3 the three mass eigenvalues and defining

$$\Delta m^2_{jk}=m^2_k-m^2_j \tag{8}$$

we therefore have that Δm^2_{12} is positive by definition, while Δm^2_{23} can have both signs, moreover, $|\Delta m^2_{23}|>\Delta m^2_{12}$. The three mixing angles are then defined in the entire first quadrant: $\theta_{jk}\in[0,\pi/2]$, while the phase is defined in the interval $\delta\in[-\pi,\pi]$. All points in this parameter space represent physically distinct solutions and parametrize an experimentally distinguishable ''neutrino world.''

For completeness we note that other conventions for the domain of variability of the mixing parameters (for the same parametrization of the mixing matrix we are using) are possible. Since s_{13} and δ enter the matrix always in the combination $s_{13}e^{-i\delta}$ and $-s_{13}e^{i\delta}$, it is possible, for example, to enlarge the domain of definition of θ_{13} to the interval $[-\pi/2,\pi/2]$, reducing the interval of definition of the phase: $\delta\in[0,\pi]$; the point $(\theta_{13},-|\delta|)$ of the conventions used in this paper is then mapped into the point $(-\theta_{13},|\delta|)$. It is also common to consider both signs of Δm^2_{12} as possible. In this case, however, the angle θ_{12} varies only in the interval $[0,\pi/4]$ with the point $(\theta_{12},-|\Delta m^2_{12}|)$ of the new convention mapped into the point $(\pi/2-\theta_{12},|\Delta m^2_{12}|)$ of our convention.

In the following discussion it will be sometimes convenient to consider a single quantity with the dimension of a

squared mass. In these cases we will use the largest squared mass difference Δm^2_{23} as a dimensional quantity and the adimensional ratio

$$x_{12}=\frac{\Delta m^2_{12}}{\Delta m^2_{23}} \tag{9}$$

to obtain the other squared mass differences: $\Delta m^2_{12}=x_{12}\Delta m^2_{23}$, $\Delta m^2_{13}=(1+x_{12})\Delta m^2_{23}$. The sign of x_{12} is equal to the sign of Δm^2_{23}.

The Super-Kamiokande data on atmospheric neutrinos [1] indicate that $|\Delta m^2_{23}|$ is in the range $2-5\times10^{-3}$ eV^2 and the angle θ_{23} is close to $\pi/4$, while θ_{13} cannot be large. Reactor experiments [3] like Chooz and Palo Verde have obtained stringent upper limits on $\sin^2 2\theta_{13}$, that together with the result of SK tell us that θ_{13} is small ($\sin^2\theta_{13}\lesssim 0.05$). The data on solar neutrinos [2] can be interpreted as evidence for oscillations, and give information on the the angles θ_{12} and Δm^2_{12} (with a constraint of θ_{13}, that has to be small in agreement with terrestrial experiments). The allowed region in the parameter space is composed of discrete regions, only one of which, the so-called large mixing angle (LMA) solution with $\Delta m^2_{12}\sim 10^{-5}-10^{-4}$ eV^2 and θ_{12} close to (but less than) $\pi/4$, gives us a reasonable chance to observe CP violation effects in ν oscillations in a standard three flavor picture.

III. THE "GEOMETRICAL" MEANING OF $|\delta|$

The three mixing angles have simple ''geometrical'' meaning in determining the overlaps $|\langle\nu_\alpha|\nu_j\rangle|^2$ between flavor and matter eigenstates: (1) The angle θ_{13} determines how much electron flavor is in the state $|\nu_3\rangle$, and how much is shared between $|\nu_1\rangle$ and $|\nu_2\rangle$ (fractions $\sin^2\theta_{13}$ and $\cos^2\theta_{13}$ respectively); (2) the angle θ_{23} describes how the nonelectron content of the state $|\nu_3\rangle$ is shared between ν_μ and ν_τ (fractions $\sin^2\theta_{23}$ and $\cos^2\theta_{23}$); (3) the angle θ_{12} describes how the electron flavor not taken by the $|\nu_3\rangle$ is shared between the $|\nu_1\rangle$ and the $|\nu_2\rangle$ (fractions $\cos^2\theta_{12}$ and $\sin^2\theta_{12}$).

It is possible and instructive to consider also the ''geometrical'' meaning of the absolute value of the phase $|\delta|$ that enters in the CP conserving part of the oscillation probabilities. For this purpose it can be useful to use a graphical representation of the mixing matrix with ''flavor boxes,'' this representation has been used before by several authors, in particular by A. Smirnov [18]. Some examples of this representation are shown in Fig. 3. Each panel in the figure shows the flavor content of the three neutrino mass eigenstates. In the three panels the values of the three mixing angles is identical, but the value of the phase δ changes. The phase $|\delta|$ determines how the muon and tau flavor not taken by the $|\nu_3\rangle$ is shared between the $|\nu_1\rangle$ and the $|\nu_2\rangle$. For $\delta=0$ the $|\nu_1\rangle$ has the largest (smallest) ν_μ (ν_τ) component, while for $\delta=\pi$ the situation is reversed. It is easy to see that the $|\langle\nu_\mu|\nu_1\rangle|^2$ overlap grows monotonically with $|\delta|$, while the $|\langle\nu_\tau|\nu_1\rangle|^2$ overlap decreases monotonically, and the opposite happens for $|\langle\nu_{\mu,\tau}|\nu_2\rangle|^2$. The range of variation is determined by the values of the three angles θ_{12}, θ_{23}, and θ_{13}.

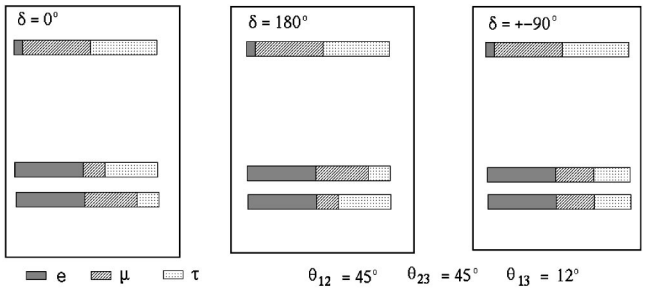

FIG. 3. Graphical representation of the flavor components of the neutrino mass eigenstates. The mixing angles have the same values in all three panels: $\theta_{12}=\theta_{23}=45°$, $\theta_{13}=12°$, the phase δ is 0, 180° and $\pm 90°$ in the left, center, and right panel. Note how the quantities $|\langle\nu_{\mu,\tau}|\nu_{1,2}\rangle|^2$ depend on the value of $|\delta|$.

In conclusion, the set of overlaps $|\langle\nu_\alpha|\nu_j\rangle|^2$ (that is, a complete solution for the flavor boxes) is equivalent to a perfect determination of the three mixing angles *and* of the value of the phase δ, but with an ambiguity of sign. The mass-flavor overlaps can be determined without ever measuring any CP or T violation effects, and therefore the absolute value $|\delta|$ can be measured without observing any such effect. Of course, mathematical consistency implies that if the determination of $|\delta|$ differs from the special values 0 or $\pm\pi$, then CP and T violation effects must exist, and we can predict their existence and their *size* but not their *sign*.

A. Quasibimaximal mixing

To illustrate our discussion with a concrete example, it can be instructive to consider in more detail the cases of ''bimaximal'' and ''quasibimaximal'' mixing. Bimaximal mixing corresponds to the values $\theta_{12}=\theta_{23}=\pi/4$ and $\theta_{13}=0$ for the mixing angles. The mixing matrix takes then the form

$$U=\begin{pmatrix} \frac{1}{\sqrt{2}} & \frac{1}{\sqrt{2}} & 0 \\ -\frac{1}{2} & \frac{1}{2} & \frac{1}{\sqrt{2}} \\ +\frac{1}{2} & -\frac{1}{2} & \frac{1}{\sqrt{2}} \end{pmatrix}. \tag{10}$$

It is well known that in this case the phase δ is physically irrelevant. In quasibimaximal mixing we allow for a small nonvanishing value of θ_{13}. In first order, that is, neglecting θ^2_{13} and approximating $c_{13}\simeq 1$, the mixing matrix becomes

$$U=\begin{pmatrix} \frac{1}{\sqrt{2}} & \frac{1}{\sqrt{2}} & s_{13}e^{-i\delta} \\ -\frac{1}{2}(1+s_{13}e^{i\delta}) & \frac{1}{2}(1-s_{13}e^{i\delta}) & \frac{1}{\sqrt{2}} \\ +\frac{1}{2}(1-s_{13}e^{i\delta}) & -\frac{1}{2}(1+s_{13}e^{i\delta}) & \frac{1}{\sqrt{2}} \end{pmatrix}. \tag{11}$$

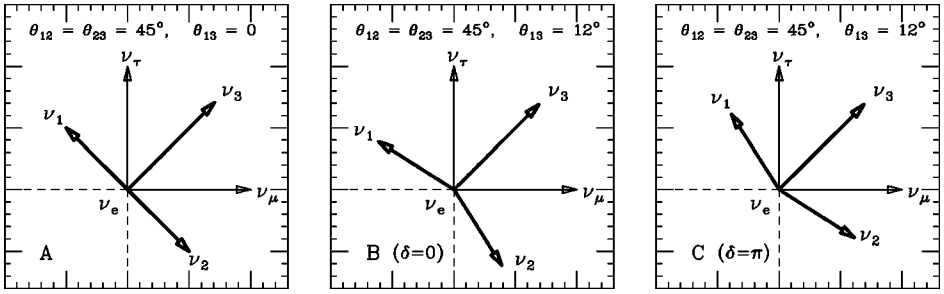

FIG. 4. Geometrical relation between the flavor and mass eigenvectors in the case of a real mixing matrix ($\delta=0$ or π). The figure shows the projections in the (ν_μ,ν_τ) plane of the mass eigenvectors. The ν_e vector is coming out of the plane of the figure. The parameters of the mixing matrix are indicated in the plots. See text for more discussion.

Note that the values of $|U_{\mu1}|$, $|U_{\mu2}|$, $|U_{\tau1}|$, and $|U_{\tau2}|$ are not fully determined by the mixing angles but can vary in the interval $[(1-s_{13})/2,(1+s_{13})/2]$. The extreme values in the interval are reached when $\delta=0$ or $\pm\pi$ and the matrix is real. It is interesting to observe that ''maximum symmetry'' (when the four elements $|\langle\nu_{\mu,\tau}|\nu_{1,2}\rangle|$ are all equal) is obtained when $\delta=\pm\pi/2$ and CP and T violating effects are largest.

For an understanding of the difference between the cases $\delta=0$ and $\delta=\pi$ it can be instructive to look at Fig. 4. The figure describes bimaximal and quasibimaximal mixing when U is a real orthogonal matrix. In this case the flavor and mass eigenstates can be represented as two sets of orthonormal vectors in ordinary 3D space. The three panels in Fig. 4 show the projections in the (ν_μ,ν_τ) plane of the mass eigenvectors. The ν_e axis is orthogonal to the plane of the paper coming out toward the reader. The left panel represents the case of bimaximal mixing: the ν_3 lies at 45° in the (ν_μ,ν_τ) plane while the vectors representing ν_1 and ν_2 are at 45° with respect to the ν_e axis coming out of the plane of the figure. The center and right panels show the projections of the vectors when θ_{13} is different from zero. In the center panel ν_3 has a small component parallel to ν_e, that is ''out'' of the plane of the figure (this corresponds to $e^{i\delta}=1$ or $\delta=0$); in the right panel ν_3 has a small component opposite to the ν_e direction (''into'' the plane, corresponding to $e^{i\delta}=-1$ or $\delta=\pi$). Performing a small rotation of the mass eigenvectors from the situation of the left panel, one can easily see the effects on the flavor components of the other mass states. For $\delta=0$ (middle panel) the ν_1 has (in absolute value) an overlap with ν_μ (ν_τ) larger (smaller) than $\frac{1}{2}$, and vice versa for ν_2. When $\delta=\pi$ (right panel) the reverse happens. Allowing the matrix U to be complex, these two discrete solutions become the two extreme cases of a continuum of possible different mixings.

B. Boxes and triangles

A graphical description of the available information on the neutrinos mixing has been introduced by Fogli and collaborators in the form of ''triangle plots'' [19]. A ''solar triangle'' plot describes the information about the mass components of $|\nu_e\rangle$: $\{|U_{e1}|^2, |U_{e2}|^2, |U_{e3}|^2\}$, while an ''atmospheric triangle'' plot describes the information about the flavor components of $|\nu_3\rangle$: $\{|U_{e3}|^2, |U_{\mu3}|^2, |U_{\tau3}|^2\}$. Each plot represents a mapping between the values of the three ν components and the points inside an equilateral triangle, each component being proportional to the distance from the point to a side of the triangle. The unitarity constraints

$$\sum_\alpha |U_{\alpha j}|^2=1 \quad \text{and} \quad \sum_j |U_{\alpha j}|^2=1 \tag{12}$$

are automatically satisfied since from elementary geometry we know that the sum of the three distances is a constant. The triangle plots allow to indicate graphically the allowed region for the three components. The element $|U_{e3}|^2$ is present in both plots and therefore there is a consistency check between the analysis of solar and atmospheric experiments. The allowed regions in the solar and atmospheric triangles carry no information about δ in the sense that when the allowed regions in both plots shrink to a single point, this is equivalent to an infinitely precise determination of the three mixing angles, with *no* information about δ [20].

More in general one can define six different ''triangle'' plots, corresponding to the three rows and columns of the mixing matrix, that is, to the mass (flavor) components of each flavor (mass) eigenstate. The set of any choice of *three* (or more) triangle plots (with one case equivalent to the set of three ''flavor boxes'') is sufficient to describe (with redundancy) all four mixing parameters including $|\delta|$, leaving, however, ambiguous the sign of the phase. To account for the sign of δ (that is, measurable only with the direct observation of CP violation effects), one of the triangles must be ''doubled.''

IV. NEUTRINO MASSES AND MIXING IN MATTER

The propagation of neutrinos in a medium differs from the vacuum case. The effects of the medium can be taken into account [21] considering an effective potential that is independent from the ν energy. In the study of flavor transitions only the difference between the potentials for different flavors is significant; in ordinary (electrically neutral) matter one has

$$V=V(\nu_e)-V(\nu_\mu)=V(\nu_e)-V(\nu_\tau)=\sqrt{2}G_F n_e, \tag{13}$$

where G_F is the Fermi constant and n_e is the electron density. The effective potential for $\overline{\nu}$ is the opposite of the ν

one: $V(\overline{\nu}) = -V(\nu)$. For neutrinos traveling close to the Earth's surface ($\rho \simeq 2.8$ g cm^{-3}, $n_e \simeq 8.4\times10^{23}$ cm^{-3}) $V \simeq 1.06\times10^{-13}$ eV, that corresponds to a length

$$V^{-1} \simeq 1850 \left(\frac{2.8 \text{ g cm}^{-3}}{\rho} \right) \left(\frac{0.5}{Y_e} \right) \text{ km} \tag{14}$$

(Y_e is the number of electrons per nucleon). The effective Hamiltonian for ν's or $\overline{\nu}$'s propagating in matter can then be written

$$\mathcal{H}(\nu) = \mathcal{H}_0 + \mathcal{H}_{\rm m}, \quad \mathcal{H}(\overline{\nu}) = \mathcal{H}_0^* - \mathcal{H}_{\rm m} \tag{15}$$

as the sum of the vacuum Hamiltonian:

$$\mathcal{H}_0 = \frac{1}{2E_\nu} U \, \text{diag}[m_1^2, m_2^2, m_3^2] U^\dagger \tag{16}$$

and a matter term that in the flavor basis (neglecting a term proportional to the unit matrix) has the form

$$(\mathcal{H}_{\rm m})_{\alpha\beta} = V \delta_{\alpha e} \delta_{\beta e} . \tag{17}$$

The effective Hamiltonian in matter can be diagonalized to obtain effective squared mass values and an effective mixing matrix in matter that will in general be different for ν and $\overline{\nu}$. The matrices $U_{\rm m}^{\nu}$, $U_{\rm m}^{\overline{\nu}}$ can be parametrized with the form (7) obtaining the parameters $\theta_{12}^{m,\nu}$, $\theta_{13}^{m,\nu}$, $\theta_{23}^{m,\nu}$, and $\delta^{m,\nu}$, and similarly for $\overline{\nu}$. The solution of this problem involves a cubic equation and can be solved analytically [22] to obtain the effective parameters as a function of the product VE_ν; however, the solution is sufficiently complex not to be particularly illuminating, and is not repeated here.

One representative example of the dependence of the effective squared masses and mixing parameters in matter on the product VE_ν is shown in Figs. 5, 6, and 7 (the density ρ is proportional to the potential V for a constant value of the electron fraction $Y_e = \frac{1}{2}$). Several important features are clearly visible most notably the ''resonance'' for the angle θ_{13} at $E_\nu \simeq |\Delta m_{23}^2|/(2V)$. More discussion is contained in Appendix C.

V. OSCILLATION PROBABILITIES IN VACUUM

The calculation of the oscillation probabilities in vacuum is a well-known problem that is briefly outlined here. The evolution equation for a neutrino state is

$$i \frac{d}{dx} \nu_\alpha = \mathcal{H}_0 \nu_\alpha = \left[\lambda \mathbf{1} + \frac{1}{2E_\nu} U \, \text{diag}[m_1^2, m_2^2, m_3^2] U^\dagger \right] \nu_\alpha , \tag{18}$$

where the Hamiltonian $\mathcal{H}_0$ has been written separating a term proportional to the unit matrix that can be dropped because it is irrelevant to the transition probabilities, m_1, m_2, and m_3 are the ν mass eigenvalues, and U is the mixing matrix. The solution of this equation for $x = L$ is

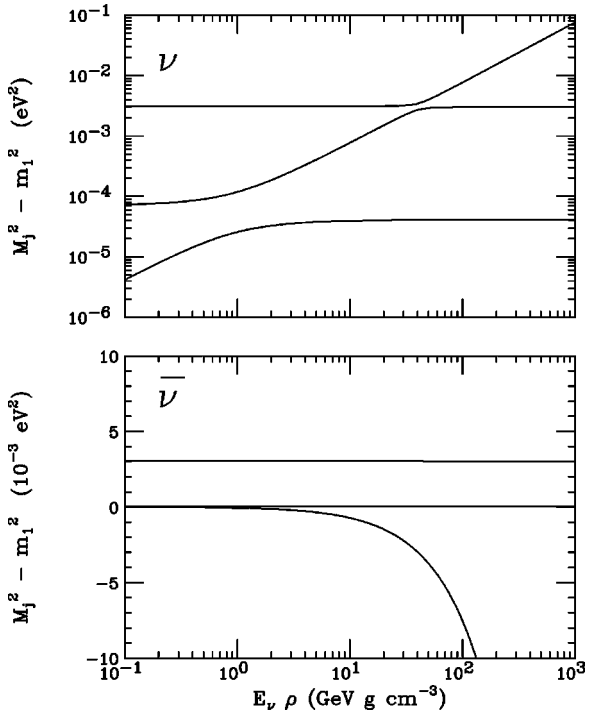

FIG. 5. Effective squared mass eigenvalues in matter, plotted as a function of $E_\nu \rho$, the top (bottom) panel is for ν ($\overline{\nu}$). The squared mass values are: $m_1^2 = 0$, $m_2^2 = 7\times10^{-5}$ eV^2, $m_3^2 = 3\times10^{-3}$ eV^2; the mixing parameters are: $\theta_{12} = 40°$, $\theta_{23} = 45°$, $\theta_{13} = 7°$, $\delta = 45°$.

$$\nu_\beta(L) = \left\{ U \exp\left(-i \frac{L}{2E_\nu} \text{diag}[m_1^2, m_2^2, m_3^2] \right) U^\dagger \right\}_{\beta\alpha} \nu_\alpha(0). \tag{19}$$

The probability for the $\nu_\alpha \to \nu_\beta$ transition ($\alpha, \beta = e, \mu, \tau$) is then

$$P(\nu_\alpha \to \nu_\beta; E_\nu, L) = \left| \sum_{j,k} U_{\beta j} \{ e^{-i(L/2E_\nu)} \, \text{diag}[m_1^2, m_2^2, m_3^2] \}_{jk} U_{\alpha k}^* \right|^2 \tag{20}$$

$$= \sum_{j,k} U_{\beta j} U_{\beta k}^* U_{\alpha j}^* U_{\alpha k} \exp\left\{ -i(m_j^2 - m_k^2) \frac{L}{2E_\nu} \right\}. \tag{21}$$

This expression can be expanded more explicitly (here and in all of the following we will always consider only nondiagonal transitions $\alpha \neq \beta$; this is no loss of generality, since the survival probabilities can be obtained from unitarity) as

$$P(\nu_\alpha \to \nu_\beta) = \frac{A_{\alpha\beta}^{12}}{2} [1 - \cos\Delta_{12}] + \frac{A_{\alpha\beta}^{23}}{2} [1 - \cos\Delta_{23}] + \frac{A_{\alpha\beta}^{13}}{2} [1 - \cos\Delta_{13}] + \pm 2J [\sin\Delta_{12} + \sin\Delta_{23} - \sin\Delta_{13}], \tag{22}$$

where

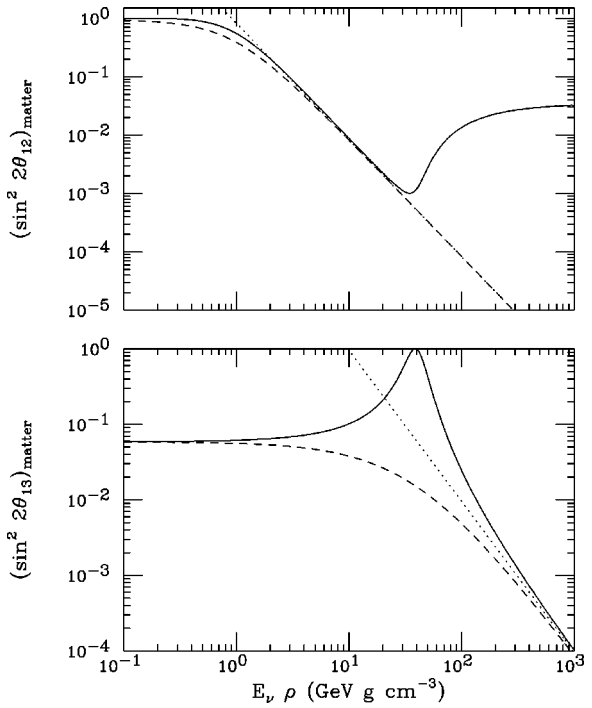

FIG. 6. Mixing parameters in matter as a function of the product $E_\nu\rho$: Top panel, $\sin^2 2\theta_{12}^{\rm m}$; bottom panel, $\sin^2 2\theta_{13}^{\rm m}$. The squared mass values are: $m_1^2=0$, $m_2^2=7\times10^{-5}$ eV^2, $m_3^2=3\times10^{-3}$ eV^2; the mixing parameters in vacuum are: $\theta_{12}=40°$, $\theta_{23}=45°$, $\theta_{13}=7°$, $\delta=45°$. The solid curves are for ν's, the dashed curves for $\overline{\nu}$'s. Note the simple asymptotic forms of the parameters for large $E_\nu\rho$. The dotted lines in the top panel are $\sin^2 2\theta_{12}[\Delta m_{12}^2/(2E_\nu V)]^2$. The dotted line in the bottom panel is $\sin^2 2\theta_{13}[\Delta m_{13}^2/(2E_\nu V)]^2$.

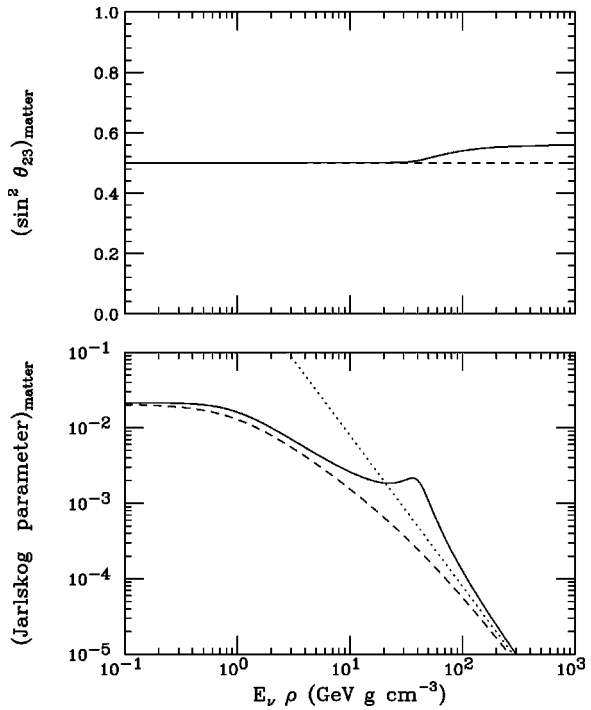

FIG. 7. Effective mixing parameters in matter plotted as a function of the product $E_\nu\rho$. The top panel shows $\sin^2\theta_{23}^{\rm m}$, the bottom panel shows the Jarlskog parameter: $J=(c_{13}^{\rm m})^2 s_{13}^{\rm m} s_{12}^{\rm m} c_{12}^{\rm m} s_{23}^{\rm m} c_{23}^{\rm m}\sin\delta_{\rm m}$. The squared mass values are: $m_1^2=0$, $m_2^2=7\times10^{-5}$ eV^2, $m_3^2=3\times10^{-3}$ eV^2; the mixing parameters in vacuum are: $\theta_{12}=40°$, $\theta_{23}=45°$, $\theta_{13}=7°$, $\delta=45°$. The solid curves are for ν's, the dashed curves for $\overline{\nu}$'s. The dotted line in the bottom panel is $J_{\rm vac}\Delta m_{13}^2\Delta m_{12}^2/(2E_\nu V)^2$ and indicates the asymptotic form of the parameter for large $E_\nu\rho$. Note how the asymptotic form is the same for ν's and $\overline{\nu}$'s.

$$\Delta_{jk}=\frac{\Delta m_{jk}^2 L}{2E_\nu}=\frac{(m_k^2-m_j^2)L}{2E_\nu}, \tag{23}$$

$$A_{\alpha\beta}^{jk}=-4\,{\rm Re}[U_{\alpha j}U_{\beta j}^* U_{\alpha k}^* U_{\beta k}], \tag{24}$$

and J is the Jarlskog [23] parameter:

$$J=J_{e\mu}^{12}=-{\rm Im}[U_{e1}U_{\mu 2}^* U_{e2}^* U_{\mu 2}] \tag{25}$$

$$=c_{13}^2 s_{13} s_{12} c_{12} s_{23} c_{23}\sin\delta, \tag{26}$$

where we have also given explicitly the expression in terms of the mixing parameters used in our convention. The contribution of the first line in Eq. (22) is symmetric under a time reversal (a replacement $\alpha\leftrightarrow\beta$) or a CP transformation (a replacement $U\leftrightarrow U^*$), while the contribution of the second line changes sign both in case of a T or CP transformation (remaining identical for CPT tranformations). The $+$ $(-)$ in Eq. (22) is valid for neutrinos (antineutrinos) when (α,β) are in cyclic order, that is, $(\alpha,\beta)=(e,\mu)$, (μ,τ), (τ,e). For (α,β) in anticyclic order the sign must be reversed. The term $[\sin\Delta_{12}+\sin\Delta_{23}-\sin\Delta_{13}]$ can also be rewritten as the product $4\sin(\Delta_{12}/2)\sin(\Delta_{23}/2)\sin(\Delta_{13}/2)$.

A. High-energy limit

It is interesting to consider the oscillation probability in the limit

$$\frac{\Delta m_{12}^2 L}{4E_\nu}\ll 1, \tag{27}$$

that is, in the approximation when the oscillations associated to the longest frequency cannot develop. If Δm_{12}^2 is in the range suggested by the solar neutrino data, the condition (27) will be satisfied in all proposed terrestrial experiments. Developing Eq. (22) in first order in Δ_{12} (and using $\Delta_{13}=\Delta_{23}+\Delta_{12}$) one obtains

$$P(\nu_\alpha\to\nu_\beta)=\frac{(A_{\alpha\beta}^{23}+A_{\alpha\beta}^{13})}{2}[1-\cos\Delta_{23}]+\frac{A_{\alpha\beta}^{13}}{2}\Delta_{12}\sin\Delta_{23}$$
$$\pm 2J\Delta_{12}[1-\cos\Delta_{23}]. \tag{28}$$

In this expression the first term is the dominant one and oscillates with the frequency $\Delta m_{23}^2/(2E_\nu)$; the other two terms are corrections proportional to $\Delta_{12}=\Delta m_{12}^2 L/(2E_\nu)$. The last term in Eq. (28) is of great interest because it describes CP and T violation effects. These effects oscillate

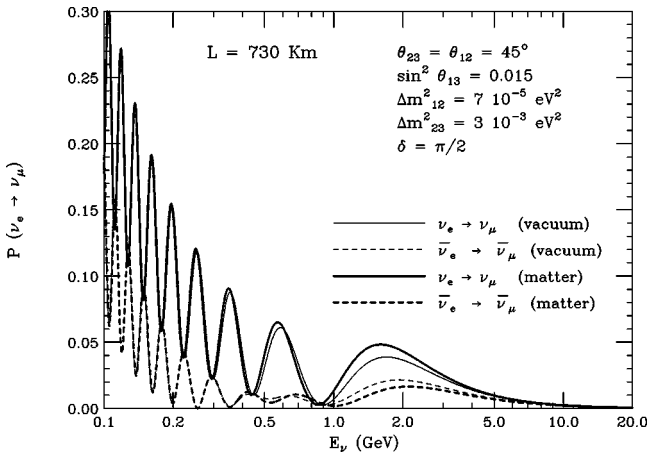

FIG. 8. Oscillation probability for the transition $\nu_e \to \nu_\mu$ plotted as a function of E_ν for a fixed value of the path length $L = 730$ km. The oscillation parameters are fixed, and are given inside the figure. The four curves are for neutrinos and antineutrinos in vacuum and in matter.

with the same frequency as the leading term, and therefore for the detection it is convenient to choose L and E_ν so that $|\Delta m^2_{23}|L/(2E_\nu) = (2n+1)\pi$ with n an integer. When this condition is satisfied the CP and T violation effects have a maximum. The amplitude of the oscillations of the CP and T violating effects is proportional to the Jarlskog parameter, and to Δm^2_{12}, therefore the possibility of the detection of CP and T violation effects is possible only if three conditions are satisfied: (1) Δm^2_{12} is sufficiently large; (2) $\sin 2\theta_{12} = 2c_{12}s_{12}$ is large; (3) θ_{13} is also large.

The first two conditions are satisfied only if the explanation to the solar neutrino problem is the LMA solution. Note also that the amplitude of the CP and T violation effects also grows as $\propto L/E_\nu$.

Examples of the oscillation probabilities $P(\nu_e \to \nu_\mu)$ and $P(\bar{\nu}_e \to \bar{\nu}_\mu)$ in the regime discussed here can be seen in Fig. 8 and in the top panels of Figs. 9 and 10 that illustrate the qualitative features discussed above.

B. Very high-energy limit

For very large E_ν (keeping L fixed), also the fast oscillations connected with the larger $|\Delta m^2_{23}|$ cannot fully develop; it is then possible to rewrite expression (22) as a power series:

$$P(\nu_\alpha \to \nu_\beta) = A_{\alpha\beta}\left(\frac{\Delta m^2_{23} L}{4E_\nu}\right)^2 + B_{\alpha\beta}\left(\frac{\Delta m^2_{23} L}{4E_\nu}\right)^3 + \cdots, \tag{29}$$

where the constants $A_{\alpha\beta}$ and $B_{\alpha\beta}$ are

$$A_{\alpha\beta} = A^{12}_{\alpha\beta} x^2_{12} + A^{13}_{\alpha\beta}(1+x_{12})^2 + A^{23}_{\alpha\beta} \tag{30}$$

and

$$B_{\alpha\beta} = \pm 8 J x_{12}(1+x_{12}). \tag{31}$$

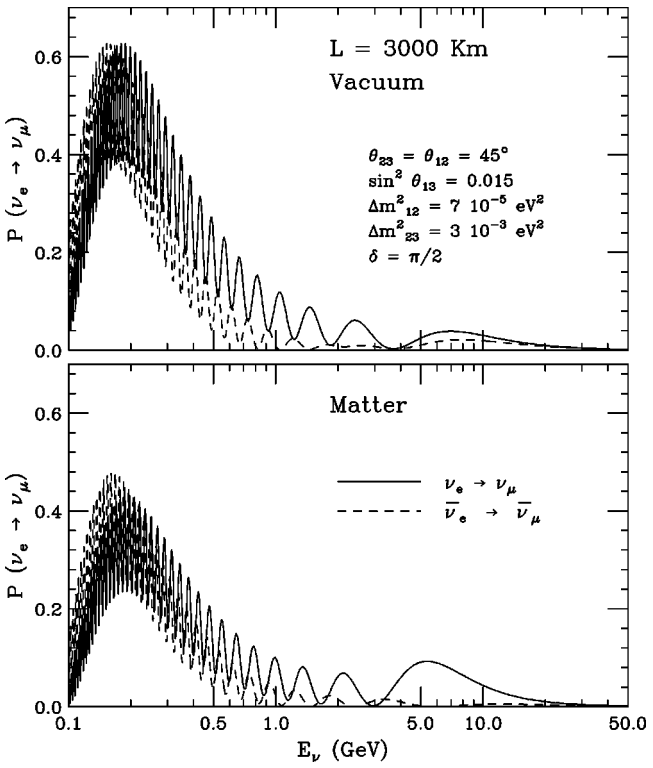

FIG. 9. Oscillation probability for the transition $\nu_e \to \nu_\mu$ plotted as a function of E_ν for a fixed value of the path length $L = 3000$ km. The oscillation parameters are fixed, and are indicated in the figure. The solid (dashed) curves are for ν ($\bar{\nu}$). The top (bottom) panel gives the probability for propagation in vacuum (matter).

Note that $A_{\alpha\beta}$ is symmetric for CP and T transformations while $B_{\alpha\beta}$ is antisymmetric.

VI. OSCILLATION PROBABILITIES IN MATTER

In this section we will develop some expressions for the oscillation probabilities in matter with constant density. The density along the trajectory of a neutrino traveling inside the Earth will change slowly, and for the interpretation of real data it will be necessary to integrate numerically the flavor evolution equation taking into account these variations, however, it is a good approximation, sufficient for the purposes of this discussion, to consider the density constant for all trajectories that do not cross the mantle-core boundary, that is, all trajectories that have $L \lesssim 1.06 \times 10^4$ km. In the approximation of constant density the problem of calculating the oscillation probabilities is elementary, in fact one can simply use the expressions developed in the previous section with the replacements $U \to U_{\rm m}$ and $m^2_j \to M^2_j$, where $U_{\rm m}$ and M^2_j the effective mixing matrix and squared mass eigenvalues in matter, that can be easily calculated as a function of the parameter $2VE_\nu = 2\sqrt{2}G_F n_e E_\nu$. The limit of this approach is that the expressions for the effective mixing parameters in matter are complicated, and the results are not transparent.

In order to gain understanding, we have calculated an

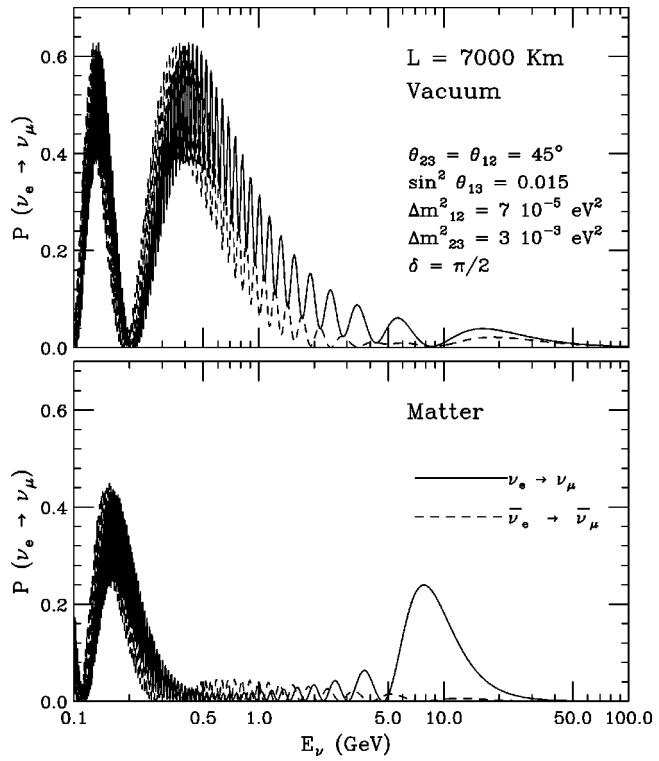

FIG. 10. Oscillation probability for the transition $\nu_e \to \nu_\mu$ plotted as a function of E_ν for a fixed value of the path length $L = 7000$ km. The oscillation parameters are fixed, and are indicated in the figure. The solid (dashed) curves are for ν ($\bar{\nu}$). The top (bottom) panel gives the probability for propagation in vacuum (matter).

expression for the oscillation probabilities that is valid in the limit of large E_ν, or more rigorously for $y = |\Delta m^2_{23}| L/(4E_\nu) < 1$. In this situation it is interesting to write down the oscillation probability as a power series in y, generalizing Eq. (29). The first three terms of this expansion are

$$P(\nu_\alpha \to \nu_\beta) = A_{\alpha\beta}\left(\frac{\Delta m^2_{23} L}{4E_\nu}\right)^2 \left[\left(\frac{2}{LV}\right)^2 \sin^2\left(\frac{LV}{2}\right)\right] + B_{\alpha\beta}\left(\frac{\Delta m^2_{23} L}{4E_\nu}\right)^3 \left[\left(\frac{2}{LV}\right)^2 \sin^2\left(\frac{LV}{2}\right)\right] + C_{\alpha\beta}\left(\frac{\Delta m^2_{23} L}{4E_\nu}\right)^3 LV \left\{\frac{48}{(LV)^4}\left[\sin^2\left(\frac{LV}{2}\right) - \left(\frac{LV}{4}\right)\sin(LV)\right]\right\} + \cdots . \quad (32)$$

The quantities $A_{\alpha\beta}$, $B_{\alpha\beta}$, and $C_{\alpha\beta}$ are adimensional constants that depend only on the ratio $x_{12} = \Delta m^2_{12}/\Delta m^2_{23}$ and the four neutrino mixing parameters. They have the important symmetry properties

$$A_{\alpha\beta} = +A_{\beta\alpha} = +A_{\overline{\alpha\beta}} = +A_{\overline{\beta\alpha}}, \quad (33)$$

$$B_{\alpha\beta} = -B_{\beta\alpha} = -B_{\overline{\alpha\beta}} = +B_{\overline{\beta\alpha}}, \quad (34)$$

$$C_{\alpha\beta} = +C_{\beta\alpha} = -C_{\overline{\alpha\beta}} = -C_{\overline{\beta\alpha}}. \quad (35)$$

Equation (32) is the main result of this paper; it is derived in Appendix A. Note that the oscillation probability (in the approximation of high E_ν) has been written as the sum of three contributions: (1) A leading contribution $\propto E_\nu^{-2}$ that is invariant for CP or T transformation; (2) a T and CP violating contribution $\propto E_\nu^{-3}$ that changes sign both for a time reversal and a CP transformation (and is therefore invariant for a CPT transformation); (3) a third contribution also $\propto E_\nu^{-3}$ that is induced by matter effects. This contribution is symmetric for a time reversal but changes sign exchanging ν with $\bar{\nu}$.

The adimensional constants $A_{\alpha\beta}$, $B_{\alpha\beta}$, and $C_{\alpha\beta}$ can be calculated from the neutrino masses and mixing: It is remarkable that the first two constants are *identical* to the coefficients in the vacuum case [Eqs. (30) and (31)]. They can be written as

$$A_{\beta\alpha} = (\mathcal{H}_0)_{\alpha\beta} (\mathcal{H}_0)^*_{\alpha\beta} \varepsilon^{-2}, \quad (36)$$

$$B_{\beta\alpha} = \mathrm{Im}[(\mathcal{H}_0)^*_{\alpha\beta} (\mathcal{H}_0^2)_{\alpha\beta}] \varepsilon^{-3}, \quad (37)$$

$$C_{\beta\alpha} = \pm \frac{1}{6} \mathrm{Re}\{(\mathcal{H}_0)^*_{\alpha\beta} [2(\mathcal{H}_0)_{\alpha e} (\mathcal{H}_0)_{e\beta} - (\mathcal{H}_0^2)_{\alpha\beta} (\delta_{\alpha e} + \delta_{\beta e})]\} \varepsilon^{-3}; \quad (38)$$

here $\mathcal{H}_0$ is the free Hamiltonian [Eq. (18)], $\varepsilon = \Delta m^2_{23}/(4E_\nu)$, and the $\pm$ sign refers to ν ($\bar{\nu}$). It can be checked that by adding to the Hamiltonian a term proportional to the unit matrix the coefficients do not change.

The three contributions to the oscillation probability have different dependences on the neutrino path length L. These dependencies are also simple power laws when L is shorter than $\sim 2V^{-1}$ (in practice when L is shorter than ~ 1500 km). Developing Eq. (32) for small VL one obtains

$$P(\nu_\alpha \to \nu_\beta) \simeq A_{\alpha\beta}\left(\frac{\Delta m^2_{23}}{4E_\nu}\right)^2 L^2 \left[1 - \frac{(VL)^2}{12} + \cdots\right] + B_{\alpha\beta}\left(\frac{\Delta m^2_{23}}{4E_\nu}\right)^3 L^3 \left[1 - \frac{(VL)^2}{12} + \cdots\right] + C_{\alpha\beta}\left(\frac{\Delta m^2_{23}}{4E_\nu}\right)^3 L^4 V \left[1 - \frac{(VL)^2}{15} + \cdots\right]. \quad (39)$$

The three contributions to the oscillation probability have dependences $\propto L^2$ for the leading term, $\propto L^3$ for the CP and T violation effects, and $\propto L^4$ for the matter induced effects.

To clarify the simple meaning of this equation let us consider an experiment with a fixed baseline L. The oscillation probabilities for the four reactions connected by CP and T transformations can be written as a power series in E_ν^{-1}:

$$P(\nu_\alpha \to \nu_\beta) = \frac{A}{E_\nu^2} + \frac{B}{E_\nu^3} + \frac{C}{E_\nu^3} + \cdots, \quad (40)$$

$$P(\nu_\beta \to \nu_\alpha) = \frac{A}{E_\nu^2} - \frac{B}{E_\nu^3} + \frac{C}{E_\nu^3} + \cdots, \tag{41}$$

$$P(\overline{\nu}_\alpha \to \overline{\nu}_\beta) = \frac{A}{E_\nu^2} - \frac{B}{E_\nu^3} - \frac{C}{E_\nu^3} + \cdots, \tag{42}$$

$$P(\overline{\nu}_\beta \to \overline{\nu}_\alpha) = \frac{A}{E_\nu^2} + \frac{B}{E_\nu^3} - \frac{C}{E_\nu^3} + \cdots. \tag{43}$$

These probabilities have a leading term that is equal for all four channels and two next order terms; one (proportional to B) that is due to the fundamental CP violation effects, and one (proportional to C) that is the result of the matter effects on the neutrino propagation. If one could excavate a tunnel along the neutrino path (to obtain vacuum oscillations) the C term in the probability would vanish, while the A and B would be modified. For $L \lesssim 3000$ km the value of A and B are approximately equal in matter and in vacuum.

In an ideal experimental program one could measure all four transitions and determine separately the coefficient A, B, and C, however, if only two channels are experimentally accessible (for example, $\nu_e \to \nu_\mu$ and $\overline{\nu}_e \to \overline{\nu}_\mu$) a single (even ideal) experiment cannot disentangle the matter effects from CP violations because they have the same functional dependence. There are several possible strategies to solve this ambiguity. One solution is to perform two experiments with different baselines. The coefficients B and C have different dependences on L (for L smaller than $2V^{-1}$ the dependences are approximately $\propto L^3$ and $\propto L^4$, respectively), and a comparison of the oscillation rates of the two experiments allow, in principle, to separate the two effects.

It can appear surprising that for large E_ν the oscillation probabilities in matter are so similar to the vacuum case, since the mixing parameters differ dramatically from the vacuum case. This is the result of some remarkable cancellations. For example, it is possible to show that the combination of parameters

$$\begin{aligned}\mathcal{F} &= J\Delta m_{12}^2 \Delta m_{23}^2 \Delta m_{13}^2 \\ &= c_{13}^2 s_{13} c_{12} s_{12} c_{23} s_{23} \sin\delta \Delta m_{12}^2 \Delta m_{23}^2 \Delta m_{13}^2\end{aligned} \tag{44}$$

is *independent* from the matter effects, that is

$$\mathcal{F}_{\mathrm{mat},\nu} = \mathcal{F}_{\mathrm{mat},\overline{\nu}} = \mathcal{F}_{\mathrm{vacuum}}. \tag{45}$$

This result has been demonstrated for the first time by Harrison, Perkins, and Scott in Ref. [24], and has the important consequence that the CP violating term of the oscillation probability is also independent from the matter effects if the ν path length L is short with respect to the three vacuum oscillation lengths ($4\pi/|\Delta m_{jk}^2|$) and the matter length $2\pi/V$. In fact,

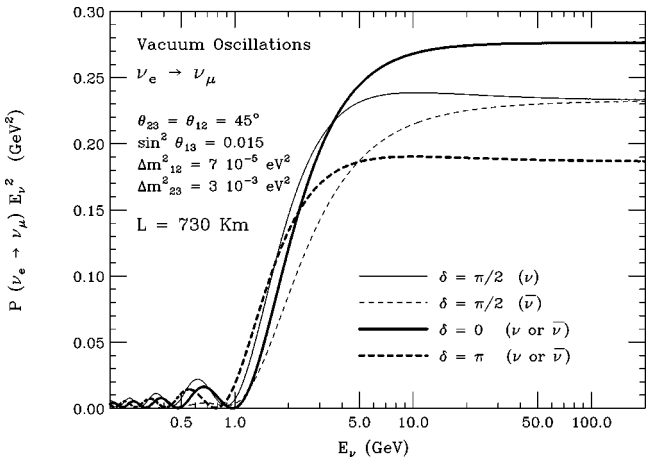

FIG. 11. In this figure we plot as a function of E_ν (for a fixed value $L = 730$ km) the product $P(\nu_e \to \nu_\mu) \times E_\nu^2$. The different curves correspond to different values of the phase δ. The values of the other parameters are indicated inside the plot.

$$\begin{aligned}\Delta P_{CP} &= 2J\left[\sin\left(\frac{\Delta m_{12}^2 L}{4E_\nu}\right)\sin\left(\frac{\Delta m_{23}^2 L}{4E_\nu}\right)\sin\left(\frac{\Delta m_{13}^2 L}{4E_\nu}\right)\right] \\ &\simeq \frac{1}{32}\frac{L^3}{E_\nu^3} J\Delta m_{12}^2 \Delta m_{23}^2 \Delta m_{13}^2 = \frac{1}{32}\frac{L^3}{E_\nu^3}\mathcal{F}.\end{aligned} \tag{46}$$

Similarly, the combinations

$$\mathcal{G}_{\alpha\beta} = A_{\alpha\beta}^{12}(\Delta m_{12}^2)^2 + A_{\alpha\beta}^{13}(\Delta m_{13}^2)^2 + A_{\alpha\beta}^{23}(\Delta m_{23}^2)^2, \tag{47}$$

where $A_{\alpha\beta}^{jk} = -4\,\mathrm{Re}[U_{\alpha j} U_{\beta j}^* U_{\alpha k}^* U_{\beta k}]$, are also independent from the matter effects.

The existence of these cancellations has been discussed in detail in Ref. [25] in the one mass-scale approximation (the limit $\Delta m_{12}^2 \to 0$). The general demonstration is technically more demanding, however, the results can be readily verified numerically. A simpler and much more interesting demonstration of these results can be obtained not by the brute force approach of comparing the product of explicit expressions to the parameters, but by using the power series expansion outlined in Appendix A.

It can be, however, interesting to see the ''magic'' of the cancellation in Eq. (45) in an explicit example that is worked out in Appendix C.

VII. DISCUSSION

Plots of the oscillation probabilities for the transitions $\nu_e \to \nu_\mu$ and $\overline{\nu}_e \to \overline{\nu}_\mu$ as a function of E_ν for three different values of the path length, $L = 730$, 3000, and 7000 km in vacuum and in matter are shown in Figs. 8, 9, and 10. To illustrate more clearly the behavior of the oscillation probability for high E_ν, in Figs. 11, 12, and 13 we show plots of the oscillation probability multiplied by E_ν^2. To compute the matter effects we have used the exact expression assuming a homogeneous medium with constant density along the ν path. Since trajectories with longer L reach deeper inside the Earth where the density is larger, the estimated average den-

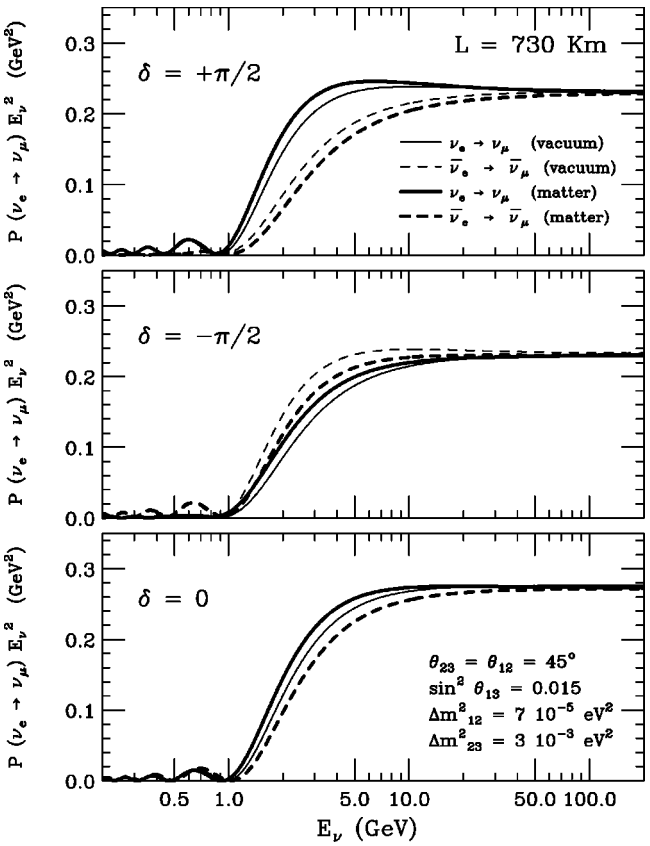

FIG. 12. In this figure we plot as a function of the neutrino energy E_ν (for a fixed value $L=730$ km) the product $P(\nu_e \to \nu_\mu) \times E_\nu^2$. The different curves describe the probability with and without matter effects.

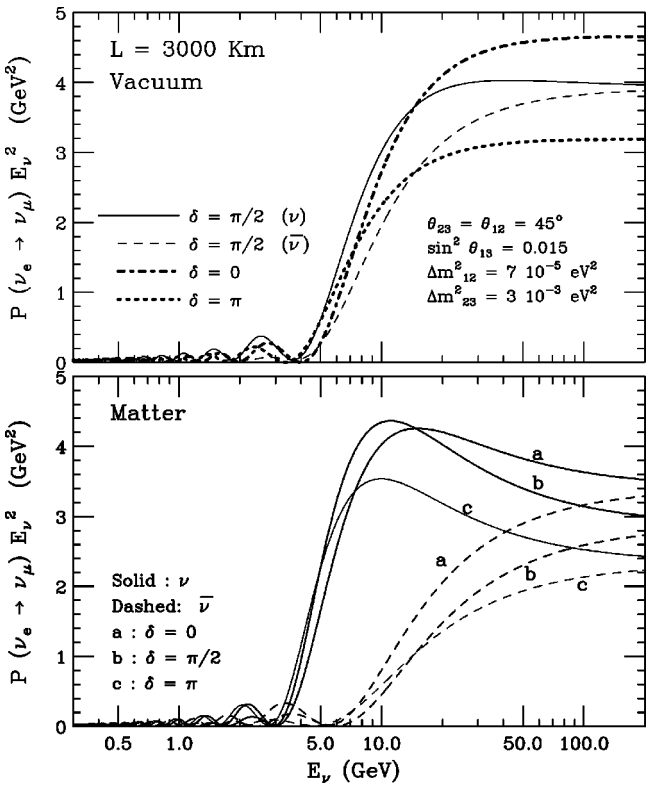

FIG. 13. In this figure we plot as a function of the neutrino energy E_ν the product $P(\nu_e \to \nu_\mu) \times E_\nu^2$, for a fixed value of the neutrino path length $L=3000$ km. The top panel is for vacuum oscillations, the bottom one includes matter effects.

sity is a function of the path length: for $L=730$, 3000, and 7000 km we have used $\rho=2.84$, 3.31, and 4.12 g cm^{-3}, always assuming an electron fraction $Y_e=0.5$. These examples exhibit a number of striking features that we will discuss in the following.

A. The measurement of θ_{13}

The focus of this work is on the measurement of *CP* violation effects, however, here are included some comments about the measurement of θ_{13}. This measurement is significantly easier, and the ''optimization'' of an experimental program is much less ambiguous than for the measurement of *CP* violation effects. It is important to stress the point that the ''optimum'' choice of L and E_μ for this measurement will not in general coincide with the optimum choice for *CP* violation studies.

The key point for this measurement is the existence of a range of E_ν where the probabilities for the $\nu_e \leftrightarrow \nu_\mu$ and $\nu_e \leftrightarrow \nu_\tau$ are enhanced because of matter effects. This enhancement, clearly visible in Figs. 9 and 10, is present for ν's if $\Delta m^2_{23}>0$ and for $\overline{\nu}$'s if $\Delta m^2_{23}<0$, therefore evidence of a nonvanishing θ_{13} should also determine the sign of Δm^2_{23} [25]. The enhancement of the transition probability is related to the existence of a Mikheyev-Smirnov-Wolfenstein (MSW) resonance for the angle θ_{13}. The effective angle $\theta^{\rm m}_{13}$ becomes in fact $\pi/4$ at an energy $E_{\rm res}$:

$$E_{\rm res} \simeq \frac{|\Delta m^2_{23}|}{2V} \cos 2\theta_{13} \simeq 14.1 \left(\frac{|\Delta m^2_{23}|}{3\times 10^{-3}\ {\rm eV}^2} \right) \left(\frac{2.8\ {\rm g\,cm}^{-3}}{\rho} \right)\ {\rm GeV}. \quad (48)$$

The position of the enhancement of the oscillation, however, does *not* coincide with the resonance energy but it is at a lower energy $E_{\rm peak}<E_{\rm res}$. There are three essential points about the matter enhancement that should be stressed.

The position of the enhancement (that is, the value of $E_{\rm peak}$) is determined to a good approximation, for small θ_{13}, only by $|\Delta m^2_{23}|$ and the path length L. The value of $E_{\rm peak}$ can be easily calculated exactly; an approximate formula that describes reasonably well the L dependence is

$$E_{\rm peak} \simeq \frac{|\Delta m^2_{23}| L}{2\pi + 2VL}. \quad (49)$$

Note that for small L this coincides with the highest energy where the vacuum oscillation probability has a maximum ($E^* = |\Delta m^2_{23}| L/2\pi$), while asymptotically (for $L \to \infty$) $E_{\rm peak} \to E_{\rm res}$.

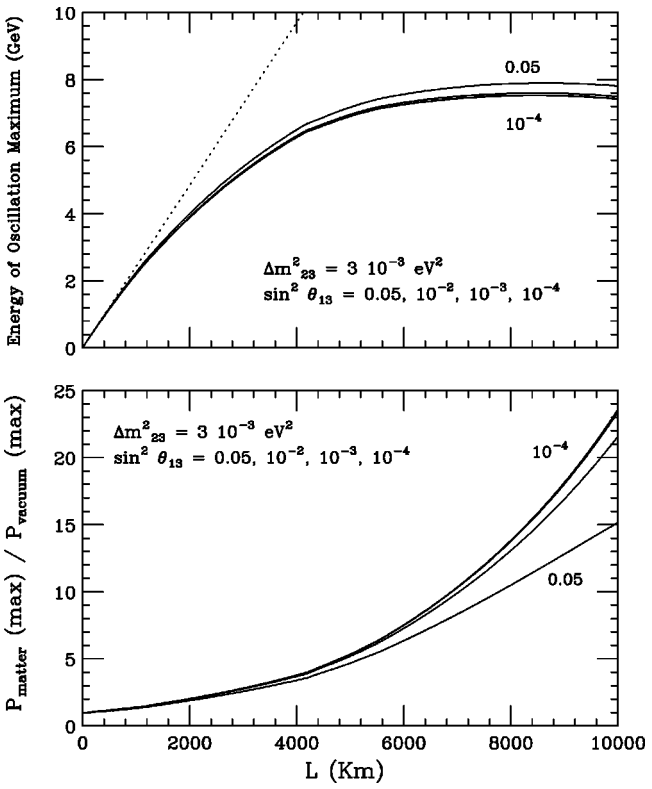

FIG. 14. The top panel shows as a function of the ν path length L the energy $E_{\rm peak}$ where the probabilities for $\nu_e \leftrightarrow \nu_{\mu,\tau}$ transitions have the matter enhanced maximum. The bottom panel shows the size of the matter enhancement. The different curves correspond to different values of s_{13}. For small s_{13} the position of the peak and the size of the enhancement are independent from s_{13}.

The size of the enhancement of the oscillation probability, in good approximation (for small θ_{13}), depends *only* on the path length L. In reasonably good approximation

$$\frac{P_{\rm peak}}{P_{\rm vacuum}} \simeq \left(1-\frac{VL}{VL+\pi}\right)^{-2} \simeq 1+\frac{2}{\pi}VL+\frac{2}{\pi}(VL)^2+\cdots . \tag{50}$$

The width of the enhancement region scales linearly with $|\Delta m^2_{23}|$.

Therefore knowing Δm^2_{23} and given the path length L of an experiment, we know *a priori* where (at what E_ν) the enhancement will be present, and also how large it will be. The value of the probability in the enhancement region is proportional to $\sin^2 2\theta_{13}$ that is unknown, and therefore is not predictable (at least without a successful theory of the ν mixing).

To illustrate these points, in Fig. 14 we plot the value of $E_{\rm peak}$ (top panel), the enhancement factor $(P_{\rm peak}/P_{\rm vac})$ for $\Delta m^2_{23}=3\times 10^{-3}$ eV^2, and several values of θ_{13} (the values of the other parameters are to a good approximation not important). It can be seen that when θ_{13} is small the curves are independent from its value.

These results can be easily understood qualitatively, since for this purpose it is sufficient to approximate $\Delta m^2_{12}\simeq 0$. In this approximation the oscillation probabilities involving electron neutrinos are proportional to the two flavor formulas (see Appendix B). The oscillation probabilities for the transitions $\nu_\mu \to \nu_e$ are then given by

$$P_{\nu_e \leftrightarrow \nu_\mu} = \frac{s^2 \sin^2\theta_{23}}{s^2+c^2(1\mp E/E_{\rm res})^2} \times \sin^2\left[\frac{\Delta m^2 L}{4E_\nu}\sqrt{s^2+c^2(1\mp E/E_{\rm res})}\right] \tag{51}$$

(where we have used the shorthand notation $s=\sin 2\theta_{13}$, $c=\cos 2\theta_{13}$). It is trivial to obtain exactly the energy E_ν of the absolute maximum of this probability and its value. The position of the maximum in general does not correspond to the the resonant energy, when the first factor is largest, because at the resonance the oscillation length becomes very long:

$$\lambda_{\rm res}=\frac{\lambda_{\rm vacuum}(E_{\rm res})}{\sin 2\theta_{13}} \tag{52}$$

(where $\lambda_{\rm vac}=4\pi E_\nu/|\Delta m^2_{23}|$ is the vacuum oscillation length) and the oscillations do not have time to develop. The maximum is found at a lower energy, where the mixing parameter is smaller but the phase of the oscillations is close to $\pi/2$.

A detailed analysis of the position of the ''peak'' in the oscillation probability and the value of the probability at the peak shows the existence of a weak dependence on the other parameters of the mixing matrix, Δm^2_{12}, θ_{12}, and δ. Therefore a careful study of the shape of the oscillation probability for the enhanced channel ($\nu_e \to \nu_\mu$ or $\overline{\nu_e}\to\overline{\nu_\mu}$ depending on the sign of Δm^2_{23}) can in principle give information on δ. This line of research is actively pursued [26]. A fundamental difficulty is that since matter effects are very large close to the resonance, they are not easy to subtract, and the uncertainties of the matter density profile along the neutrino path can be reflected into effects on the probability of the same size as the CP violation effects.

B. The "vacuum mimicking" region

Looking at Fig. 8 one can note a remarkable feature, namely, the fact that the oscillation probabilities for $L=730$ km and $E_\nu \lesssim 0.5$ GeV are approximately independent from the presence of matter. This phenomenon has been observed before, in particular by Minakata and Nunokawa [11], who refer to it as ''vacuum mimicking.'' At first sight the closeness of the oscillations in matter and vacuum for energies as large as 0.5 GeV traveling in ordinary matter may seem surprising, since we can expect, and indeed it is the case, the effective squared mass values and mixing parameters are modified by the matter potential, however, these modifications of the oscillation parameters are *not* reflected in the oscillation proabilities if the neutrino path length is sufficiently short, namely if $VL \ll 1$. In fact it can be proved (see Appendix A) that the difference $\Delta P_{\rm matter}=P_{\rm matter}-P_{\rm vacuum}$ (for a homogeneous medium) can be expressed as a power series in VL and becomes negligible for VL small no matter how different from the vacuum values are the ef-

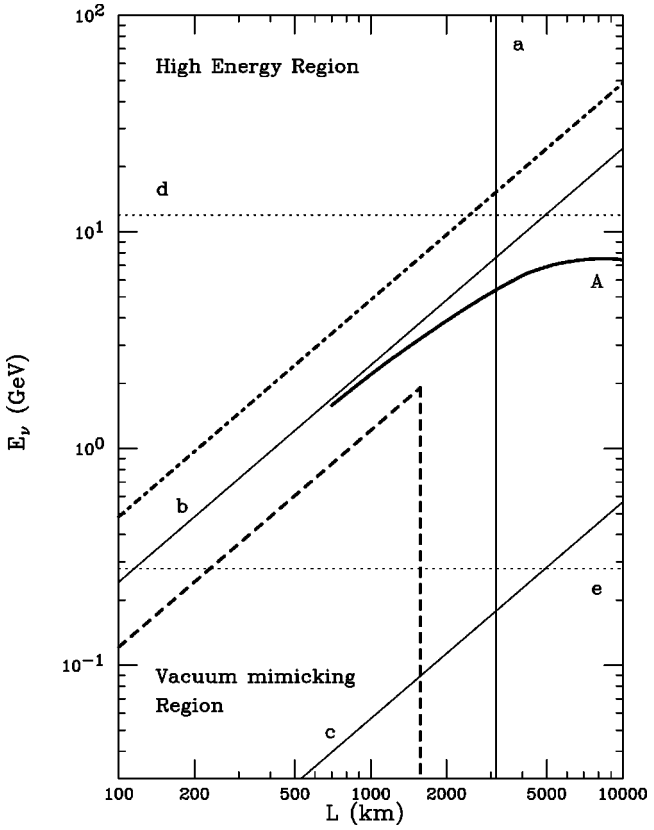

FIG. 15. In this figure are indicated some interesting regions in the space (L,E_ν) of the oscillation probability for $\nu_e \leftrightarrow \nu_\mu$ and $\nu_e \leftrightarrow \nu_\tau$ transitions. The region above the dot-dashed line is the one where the high-energy expansion is valid. In the region delimited by the dashed line the oscillation probabilities in matter and in vacuum are to a good approximation equal. The line labeled *A* shows the ν energy where the oscillation probability has the largest matter induced enhancement. The line is drawn only if the maximum enhancement is larger than 20%. The line labeled with *a* shows the relation $L=2V^{-1}$ for the Earth's crust ($\rho=2.8\ \mathrm{g\,cm^{-3}}$). The lines *b* and *c* show the relations $E_\nu=|\Delta m^2_{23}|L/(2\pi)$ and $E_\nu=\Delta m^2_{12}L/(2\pi)$, that is, the highest energy where the oscillation probability has a maximum. Line *d* indicates the approximate energy for which θ_{13} passes through a resonance, and line *e* shows the energy above which matter effects modify significantly the mixing parameters.

fective squared masses and mixing parameters that correspond to the product VE_ν parameters.

This is illustrated in Fig. 15 which describes different regions in the plane (L,E_ν) where the oscillation probabilities for the $\nu_e \leftrightarrow \nu_{\mu,\tau}$ transitions have different qualitative properties. The figure is constructed for $\Delta m^2_{23}=3\times10^{-3}$ eV^2, $\Delta m^2_{12}=7\times10^{-5}$ eV^2, and for the potential $V=1.06\times10^{-3}$ eV (that corresponds to the Earth's crust).

(1) The effects of matter on the oscillation probability can be significant only if L is close or larger than $2V^{-1}$ that is close or to the right of the line labeled *a*. For growing L the matter effects become more and more important (compare Figs. 8, 9, and 10) and a more and more serious background for CP violation studies.

(2) Curve *b* is defined by $E_\nu=|\Delta m^2_{23}|L/(2\pi)$, and indicates the position of the highest energy maximum of the transition probabilities; above this line they decrease monotonically without further oscillations.

(3) Curve *c* is defined by the relation $E_\nu=\Delta m^2_{12}L/(2\pi)$ and gives the highest energy where the slow (''solar'') vacuum oscillations have a maximum.

(4) Matter effects are particularly spectacular for $E_\nu \simeq |\Delta m^2_{23}|/(2V)$ (curve *d*) when θ_{13} undergoes an MSW resonance.

(5) The matter effects have negliglible effects on the effective squared masses and mixing (and therefore no effect on the transition probabilities) if $E_\nu \ll \Delta m^2_{12}/(2V)$ (curve *e*). For $\theta_{12}\neq\pi/4$ this corresponds also (adding a factor $\cos 2\theta_{12}$) to the location of the MSW resonance for the angle θ_{12}.

(6) The ''high-energy region'' that is the main focus of this work corresponds to the region above the thick dot-dashed lines, when the probability is not oscillating any more.

(7) The ''vacuum mimicking region'' corresponds to the short path length (significantly shorter than $2V^{-1}\simeq3700$ km. In order to access CP (T) violation effects where they are large, the energy must also be small enough to see the development of several oscillations. This qualitatively corresponds to the region delimited by the thick dashed line.

(8) Finally the thick curve labeled *A* indicates the energy where the MSW enhancement (or suppression) of the probability is most important (corresponding to E_{peak} discussed in the previous subsection. The line is plotted only when the enhancement of the probability is larger than 20%. The enhancement becomes more and more important with growing L [see Eq. (50)]. The best place to search for a nonvanishing θ_{13} is close to this line.

C. High-energy neutrinos

We will now discuss in more detail the behavior of the oscillation probabilities for high E_ν when they are monotonically decreasing. Some important features of the oscillation probability in vacuum, illustrated in Fig. 11, show the product $P_{\nu_e\to\nu_\mu}\times E^2_\nu$ plotted as a function of E_ν for a fixed value $L=730$ km: (1) For large E_ν the oscillation probability is well approximated with the form A/E^2_ν; (2) the value of the constant A (keeping all other parameters fixed) depends on the value of the $\cos\delta$ (this is a crucial remark); (3) the CP violation effects (present when $\sin\delta\neq0$) have an energy dependence $\propto E^{-3}_\nu$.

Figure 12 illustrates how the oscillation probability is modified by the matter effects (for the same $L=730$ km and the same ν masses and mixing as the previous figure). The probabilities in vacuum and in matter for the longer path length $L=3000$ km are shown in Fig. 13. Some important points are the following: (1) Matter effects generate a $\nu/\overline{\nu}$ asymmetry; (2) the matter induced asymmetry has the same energy dependence ($\propto E^{-3}_\nu$) as the one generated by the fundamental CP violation effects; (3) the effects of the phase δ

and of matter can both contribute to the observable $\nu/\bar{\nu}$ asymmetry, either adding or subtracting from each other; (4) the effects of matter depend strongly on the path length L; (5) the relative importance of the matter induced asymmetry with respect to the asymmetry generated by the fundamental CP violation effects grows approximately linearly with L [see Eqs. (32) and (39)], and the ''background'' of the matter induced asymmetry is a much more serious problem at $L=3000$ km; (6) the effect of the presence of matter on the leading-order term (A/E_ν^2) of the transition probability also depend on the path length L (i) for short L the constant in matter $A_{\rm mat}$ is equal to the vacuum value $A_{\rm vac}$, (ii) for longer L $(L \gtrsim 2V^{-1})$ the leading term of the oscillation probability is suppressed [see again Eqs. (32)]; however, one has $A_{\rm mat}=F(LV)\times A_{\rm vac}$, that is, the constant A is proportional to the vacuum value with a proportionality factor that depends only on the product of VL; therefore a measurement of the leading term again carries information about $\cos\delta$.

D. The leading term in the oscillation probability and $|\delta|$

The leading term in the oscillation probability $\sim A_{\alpha\beta}/E_\nu^2$ is equal for all the four transitions related by a CP or a T transformation, however, in principle its measurement, together with a precise determination of the other oscillation parameters, can give information about the phase δ. In fact, most of the sensitivity to δ claimed by recent analysis of the potential of high energy ν factories, is essentially the result of a high precision measurement of the constant A. Considering all other parameters as fixed and Δm^2_{23} positive, the constant $A_{e\mu}$ is largest when $\delta=0$, and decreases monotonically with growing $|\delta|$, reaching a minimum value for $|\delta|=\pi$. Conversely $A_{e\tau}$ is maximum for $|\delta|=\pi$ and minimum for $\delta=0$. For $\Delta m^2_{23}<0$ the dependence of $A_{e\mu}$ and $A_{e\tau}$ on $|\delta|$ is reversed.

It is simple to give a qualitative explanation for this behavior. The constant $A_{\alpha\beta}$ can be expressed as the sum of three contributions each one associated to a squared mass difference:

$$A_{\alpha\beta}=A^{12}_{\alpha\beta}\times x_{12}^2+A^{13}_{\alpha\beta}\times(1+x_{12})^2+A^{23}_{\alpha\beta}\times 1. \quad (53)$$

In this expression each factor $A^{jk}_{\alpha\beta}=-4\,\mathrm{Re}[U_{\alpha j}U^*_{\alpha k}U^*_{\beta j}U_{\beta k}]$ is weighted proportionally to to the square of the relative squared mass difference Δm^2_{jk}. The general expressions for the different terms in our parametrization of the mixing matrix are easily calculated. For the $\nu_e\leftrightarrow\nu_\mu$ transitons one has

$$A^{12}_{e\mu}=4s^2_{12}c^2_{12}c^2_{13}(c^2_{23}-s^2_{13}s^2_{23})+(c^2_{12}-s^2_{12})s_{13}s_{23}c_{23}\cos\delta, \quad (54)$$

$$A^{13}_{e\mu}=4s^2_{13}c^2_{13}s^2_{23}c^2_{12}+4s_{12}c_{12}s_{13}c^2_{13}s_{23}c_{23}\cos\delta, \quad (55)$$

$$A^{23}_{e\mu}=4s^2_{13}c^2_{13}s^2_{23}s^2_{12}-4s_{12}c_{12}s_{13}c^2_{13}s_{23}c_{23}\cos\delta. \quad (56)$$

One can see that the term $A^{12}_{e\mu}$ is nonvanishing also for $s_{13}=0$, and in fact is related to the ''solar oscillations.'' Note also that the sum $A^{13}_{e\mu}+A^{23}_{e\mu}$ is independent from δ (and from θ_{12}), however, the two individual terms do depend on the phase (and also on θ_{12}). For $\cos\delta\to 1$ the term $A^{13}_{e\mu}$ becomes largest while $A^{23}_{e\mu}$ becomes smallest; this is a consequence of the fact that the overlap $|\langle\nu_\mu|\nu_1\rangle|$ is largest for $\cos\delta=1$ (see discussion in Sec. III). This has simple but important consequences when considering the combination (53). When x_{12} is positive (that is for Δm^2_{23} positive) one has $|\Delta m^2_{13}|>|\Delta m^2_{23}|$ and the contribution A^{13} receives the largest weight, therefore the e-μ oscillations have the highest probability when $A^{13}_{e\mu}$ is largest that is when $\cos\delta=1$. For x_{12} negative $(\Delta m^2_{23}<0)$ one has $|\Delta m^2_{13}|>|\Delta m^2_{12}|$ and therefore it is the term A^{23} that receives the larger weight, therefore the probability is largest when A_{23} is largest, that is for $\cos\delta=0$. A similar discussion can be performed for e-τ transitions. In this case the oscillation probability is largest when $\cos\delta=0$ for $\Delta m^2_{23}>0$, and when $\cos\delta=1$ for $\Delta m^2_{23}<0$.

For a simple illustration we can consider the case of quasibimaximal mixing $(\theta_{23}=\theta_{13}=\pi/4)$. Keeping only terms in first and second order in s_{13} one obtains

$$A_{e\mu,e\tau}=\frac{1}{2}(1-s^2_{13})x^2_{12}+2s^2_{13}+s_{13}\cos\delta[(1+x_{12})^2-1]. \quad (57)$$

One can recognize three main contributions that can be considered as the ''solar contribution,'' the ''θ_{13} contribution,'' and the ''mass splitting effect.''

(1) The first term $\propto x^2_{12}$, is due to the effect of oscillations involving only the states ν_1 and ν_2. This contribution is nonvanishing also for $\theta_{13}=0$, it is ''guaranteed'' to exist, since it is responsible for the oscillations of solar neutrinos.

(2) The second contribution $\propto s^2_{13}$, can be understood as oscillations between the state ν_3 and the quasidegenerate pairs ν_1-ν_2. This contribution is independent from the solution of the solar neutrino problem and can in fact exist also for $\Delta m^2_{12}\to 0$, however, it can be arbitrarily small since it is proportional to s^2_{13} for which exists only an upper limit.

(3) The third contribution is $\propto s_{13}x_{12}\cos\delta$, and is nonvanishing only if both Δm^2_{12}, and s_{13} are nonzero. It arises as the consequence of the different weights for the oscillations ''between'' the pairs of states ν_1-ν_3, or ν_2-ν_3 due to the associated squared mass difference. This is the contribution that carries information about the phase δ.

An important remark is that, for a large interval of values, when s_{13} decreases it becomes *easier* to measure the contribution of the $\cos\delta$ term, even if it becomes smaller. This happens because the leading contribution is usually the ''θ_{13} term'' that is $\propto s^2_{13}$ and decreases quadratically with s_{13}, while the $\cos\delta$ contribution decreases only linearly with s_{13}. In fact, Cervera *et al.* [15] in their analysis of the sensitivity of ν-factory experiment have found (see Fig. 22 in their work) that the range of Δm^2_{12} where it is possible to distinguish $\delta=0$ and $\delta=\pi/2$ is approximately constant (with actually a small *increase*) when θ_{13} becomes smaller, down to the smallest angles they investigated. This observation seems a paradox, since the CP violation effects decrease linearly with s_{13}. However, the observation is correct, and can be easily understood with the argument outlined above. If the

authors of Ref. [15] had studied the possibility to discriminate between $\delta=-\pi/2$ and $\delta=+\pi/2$ the allowed region would be significantly smaller, and shrink linearly with θ_{13}. This in fact reveals the conceptual difference between measuring *CP* violation effects and measuring the phase δ.

In summary:

(1) The measurement of the leading term in the oscillation that is a quantity symmetric under *CP* and *T* transformations gives information about the value of $\cos\delta$. This result does not allow us to determine the sign of the *CP* violation effects.

(2) A precise measurement of the leading term in the oscillation probability is significant as a measurement of $|\delta|$ only if the other oscillation parameters can be measured separately with a sufficient accuracy. The requirement on the precision of the measurements of the ''solar parameters'' θ_{12} and Δm^2_{12} are particularly stringent [they can be deduced from Eqs. (53)–(57)].

VIII. CONCLUSIONS

In this work we have addressed the question of the optimum strategy, that is, the best choice of ν energy and path length, to measure the two remaining completely unknown parameters in the neutrino mixing matrix [27], that is, the angle θ_{13} and the phase δ.

For the measurement of θ_{13} it is possible to make a strong case for a high E_ν and long L program. The oscillation probability for the $\nu_e\leftrightarrow\nu_\mu$ (or $\bar{\nu}_e\leftrightarrow\bar{\nu}_\mu$ depending on the sign of Δm^2) transitions will be enhanced in a well defined and precisely predictable energy range. It is in this energy range that the search for the effects of a nonvanishing θ_{13} has the best possibilities. The maximum of the oscillation probability corresponds to an energy $E_{\rm peak}$ that is proportional to $|\Delta m^2_{23}|$, is only weakly dependent on Δm^2_{12} and the mixing parameters, and grows with increasing L in a well defined way [see Eq. (49) and the following discussion]. For $|\Delta m^2_{23}|=3\times10^{-3}$ eV^2 $E_{\rm peak}$ is approximately 1.6, 5.2, and 7.4 GeV for $L=730$, 3000, and 7000 km. The value of the probability at $E_{\rm peak}$ can be predicted as $P^{\rm max}_{\nu_e\leftrightarrow\nu_\mu}\simeq\sin^2 th2\theta_{13}\sin^2\theta_{23}\times F$ where F is a matter enhancement effect that to a good approximation depend *only* on the path length L [see Eq. (50)]. For $L=730$, 3000, and 7000 km the enhancement F is $\sim$1.25, 2.8, and 10.3. The best strategy for a detection of θ_{13} is therefore to use a very long path length (since it improves the signal to background) and design a neutrino beam with maximum intensity in the energy range where the probability is predicted to have the maximum. Note that for this study, a conventional beam [28,29] could be competitive with a neutrino factory.

The study of *CP* and *T* violation effects is a fascinating subject, and it is remarkable that if two conditions are satisfied, (i) the LMA solution is the explanation of the solar neutrino problem, and (ii) θ_{13} is sufficiently large, these effects are in principle observable with accellator ν beams, and the phase δ is experimentally measurable; however, these are extraordinarily difficult tasks, and the best strategy is not easily determined. Very likely in this case the very well controlled and intense beams of a ν factory are a uniquely well suited tool; however, the choice of E_μ and L is not a simple decision. A large E_μ allows very high event rates, but results in high-energy neutrinos that have small oscillation probabilities and for which the *CP* violation effects are strongly suppressed ($\propto E_\nu^{-3}$), moreover, the matter effects become a more dangerous source of background.

To analyze quantitatively if the high rates of a high-energy neutrino factory are sufficient to extract information about the phase δ we have analyzed in detail the oscillation probabilities for high-energy neutrinos, expressing the probability as a power series expansion in the adimensional parameter $y=|\Delta m^2_{23}|L/(4E_\nu)$. This expansion is useful when y is less than unity, that is, for E_ν larger than few GeV, even for the largest possible L, and reveals several important features of the probability. Keeping only the lowest order terms in the expansion, the oscillation probabilities is the sum of three contributions:

$$P=A_0(\cos\delta)\frac{L^2}{E_\nu^2}\pm B_{CP}\sin\delta\frac{L^3}{E_\nu^3}\pm C_{\rm mat}V\frac{L^4}{E_\nu^3}. \qquad (58)$$

One can distinguish: (1) a leading-order contribution $\propto E_\nu^{-2}$, that is symmetric under *CP* and *T* transformation; (2) a *CP* and *T* antisymmetric contribution of order E_ν^{-3}, that depends linearly on $\sin\delta$; (3) a matter induced contribution, also proportional to E_ν^{-3}, that is invariant for a *T* reversal transformation, but changes sign replacing ν with $\bar{\nu}$ (or vice versa). This term is proportional to the potential V and vanishes in vacuum.

It is important to note the L dependence of the three terms: longer L enhances the *CP* violation effects, but enhances more dramatically the matter effects.

The largest effect of the phase δ is on the leading term coefficient A. This coefficient can be measured with great precision, and for this purpose a very high energy is the optimum solution, however, the value of $\cos\delta$ extracted from the measurement only if the squared mass differences and mixing angles are determined (from other measurements) with sufficient precision. The possibility to obtain the required accuracy for the solar parameters θ_{12} and Δm^2_{12} is problematic and should be critically analyzed.

The detection of a genuine *CP* violation effect is more difficult. It requires first of all to subtract the matter induced asymmetry. This can be done having two experiments with different baselines, and using the different L behavior of the two contributions, or studying the energy dependence of the probability down to lower E_ν. Note that the effect on the event rate induced by the fundamental *CP* violation is constant with increasing E_μ, since the increase in the rate $\propto E_\mu^3$ is compensated by the suppression in the probability $\propto E_\nu^{-3}$ for higher energy neutrinos. Since the backgrounds increase with energy, the optimum solution for the search of the asymmetry is not an arbitrary high energy.

The distinction between the measurement of *CP* violation effects and the measurement of the phase δ has also been stressed in Ref. [12].

The authors of some recent works [15,16] on the sensitivity of high-energy neutrino factories for the determination of δ have neglected to consider the entire interval of definition of the phase $\delta \in [-\pi, \pi]$, studying only the positive semi-interval. It would be interesting to see a reanalysis of those works that considers the entire interval of definition for δ. The outcome should be that at least in a significant part of the parameter space an input value $\delta_{\rm input}$ can be reconstructed with fits of approximately the same quality as $\delta_{\rm rec} \sim \delta_{\rm input}$ and $\delta_{\rm rec} \sim -\delta_{\rm input}$. This would reveal how much of the sensitivity is coming from the measurement of the CP violating part of the oscillation probability, and how much is coming from the high precision measurement of the CP conserving part.

An ambiguity of sign in the dermination of δ leaves ambiguous also the sign of all CP of T violation effects in the neutrino sector. This can obviously be a limitation, for example, for a discussion of the relation between these effects and the observed CP asymmetry of the present universe. More in general, it should be noted that a measurement of $\cos\delta$ is not rigorosly speaking a measurement of CP violations at all, but it implies the existence of CP violations of predicted size but unknown sign. One point that in my opinion would require more attention is the following, the measurement of $\cos\delta$ (different from the special values 0 and 1) is equivalent to the statement that three flavors, two squared mass differences, and three mixing angles are insufficient to describe all observed results about the ν flavor transitions, and that the inclusion of a new parameter can reconcile all results. It is not clear if this interpretation of the data would be unique. It is interesting to discuss if other mechanisms, for example the introduction of new neutrino properties (such as FCNC interactions) or additional small mixings (''LSND like'') with light sterile states, could also be viable descriptions of the data.

An experimental program with low-energy neutrinos and a short path length has, in principle, some very attractive features: (i) the problem of disentangling the matter effects is much less severe because these effects are small, (ii) a direct measurement of CP violation effects is possible, (iii) the oscillation probability can have more structure, and the CP violation effects can be very large (with $\Delta P_{CP}/P \sim 1$). Unfortunately, the experimental difficulties are enormous, because of poor focusing, small cross sections, and the experimental difficulty of flavor determination. The question of which one of the two options (high energy or low energy) is more promising for the measurement of the phase δ and of CP violation effects for leptons remains in my view still open, and more detailed studies have still to be performed.

ACKNOWLEDGMENTS

This work was initiated by conversations with Alain Blondel, Andrea Donini, Belen Gavela, Michael Lindner, and Hisakazu Minakata. I am very grateful to Maurizio Lusignoli and Andrea Donini for several discussions and the kind reading of an early version of this work. Lively discussions with Hisakazu Minakata, Hiroshi Nunokawa, and Osamu Yasuda are gratefully acknowledged.

APPENDIX A: OSCILLATION PROBABILITIES AS POWER SERIES

Oscillations in vacuum

In this appendix we will show how the ν oscillation probabilities both in vacuum and in homogeneous matter can be expressed as a power series.

We can start with the vacuum case. In this case, as discussed in Sec. V, the oscillation probabilities can be calculated with simple analytical formulas and are a function of the ratio L/E_ν. It is useful to define the adimensional quantity y:

$$y = \frac{\Delta m^2_{23} L}{4 E_\nu}. \tag{A1}$$

It is straightforward to expand the oscillation probability as a power series in y:

$$P_{\alpha\to\beta}(L, E_\nu) = \sum_{n=2}^{\infty} c_n^{\alpha\to\beta} y^n, \tag{A2}$$

developing in a Taylor series the trigonometric functions in the analytic expression (22). The constants $c_n^{\alpha\to\beta}$ are adimensional quantities that can be written as functions of the squared mass ratio $x_{12} = \Delta m^2_{12}/\Delta m^2_{23}$ and of the four mixing parameters. The expansion (A2) is formally always valid, it is of course useful only when y is less than unity, that is, for short ν path length or high E_ν. Since the expansion of the cos (sin) function that describe the CP conserving (violating) part of the probability has only even (odd) powers of their argument, the coefficients have the following symmetry properties:

$$\begin{aligned} c_n^{\alpha\to\beta} &= +c_n^{\beta\to\alpha} = +c_n^{\bar\alpha\to\bar\beta} = +c_n^{\bar\beta\to\bar\alpha} \quad \text{for } n \text{ even}, \\ c_n^{\alpha\to\beta} &= -c_n^{\beta\to\alpha} = -c_n^{\bar\alpha\to\bar\beta} = +c_n^{\bar\beta\to\bar\alpha} \quad \text{for } n \text{ odd}. \end{aligned} \tag{A3}$$

Note in particular that the lowest order (leading) term of the expansion is exactly CP conserving, while the next term is CP antisymmetric. It follows that the determination in an experiment with a fixed baseline, that the flavor transition probability in vacuum vanishes at high energy with the form $P_{\nu_\alpha\to\nu_\beta} \simeq a E_\nu^{-2} + b E_\nu^{-3}$ with $b \neq 0$, would be a proof of the existence of CP violations in the neutrino sector.

It is useful to rederive the expansion (A2) of the oscillation probability with a different method, that can be more easily extended to the case of neutrinos propagating in matter. The S matrix for flavor transition can be calculated as

$$S(\nu_\alpha \to \nu_\beta) \equiv S_{\beta\alpha} = \exp[-i\mathcal{H}_0 L]_{\beta\alpha}, \tag{A4}$$

where $\mathcal{H}_0$ is the free Hamiltonian. The S matrix for the transitions of $\bar\nu$'s can be obtained replacing $\mathcal{H}_0$ with the complex conjugate $\mathcal{H}_0^*$. Expanding the exponential one has

$$S_{\beta\alpha}=\exp[-i\mathcal{H}_0L]_{\beta\alpha}=\delta_{\beta\alpha}+(-iL)(\mathcal{H}_0)_{\beta\alpha}+\frac{1}{2!}(-iL)^2(\mathcal{H}_0^2)_{\beta\alpha}+\cdots. \tag{A5}$$

The transition probability can be obtained by squaring the corresponding matrix element:

$$P_{\alpha\to\beta}=|S_{\beta\alpha}|^2. \tag{A6}$$

Collecting all terms proportional to L^n for each integer n, one can then obtain the probability as a power series in L. This actually corresponds to the powers series in y, since L always enters in the combination $\mathcal{H}_0L$ or $\mathcal{H}_0^*L$, and the Hamiltonian can be written (neglecting a term proportional to the unit matrix) as

$$\mathcal{H}_0=\frac{\Delta m_{23}^2}{4E_\nu}U\,\mathrm{diag}[-(1+2x_{12}),-1,1]U^\dagger=\frac{\Delta m_{23}^2}{4E_\nu}\hat{h} \tag{A7}$$

and each power of $\mathcal{H}_0$ (or $\mathcal{H}_0^*$) contributes a factor $\Delta m_{23}^2/(4E_\nu)$. Writing explicitly the lowest order terms one finds

$$P_{\beta\to\alpha}=[\hat{h}_{\alpha\beta}\hat{h}_{\alpha\beta}^*]y^2+\mathrm{Im}[\hat{h}_{\alpha\beta}^*(\hat{h}^2)_{\alpha\beta}]y^3+\cdots \tag{A8}$$

from where we can read the expressions for $c_2^{\alpha\to\beta}$ and $c_3^{\alpha\to\beta}$. The symmetry properties of the coefficients can be easily checked: (1) the lowest order term ($\propto y^2$) of the probability is symmetric for time reversal, since $\mathcal{H}_0$ is an Hermitian matrix: $(\mathcal{H}_0)_{\alpha\beta}=(\mathcal{H}_0)_{\beta\alpha}^*$; (2) the leading term is also symmetric for a CP transformation since in this case one has to replace the Hamiltonian $\mathcal{H}_0$ with its complex conjugate; (3) the next to leading term $\propto y^3$ is antisymmetric under a CP or T transformation as can be immediately deduced from the fact that $\mathcal{H}_0$ is Hermitian.

The coefficients $|\hat{h}_{\alpha\beta}|^2$ and $\mathrm{Im}[\hat{h}_{\alpha\beta}^*(\hat{h}^2)_{\alpha\beta}]$ can be easily written in terms of the mixing parameters and the squared mass ratio x_{12} verifying that the expansion (A8) is identical to the one given in Eq. (29).

Oscillations in matter

The effective Hamiltonians describing the flavor evolutions of ν's and $\bar{\nu}$'s in matter can be written as

$$\mathcal{H}_\nu L=\mathcal{H}_0L+\hat{p}_eVL=\hat{h}y+\hat{p}_ez, \tag{A9}$$

$$\mathcal{H}_{\bar{\nu}}L=\mathcal{H}_0^*L-\hat{p}_eVL=\hat{h}^*y-\hat{p}_ez, \tag{A10}$$

where we have introduced the ν_e projection operator $\hat{p}_e$ [with the property $(\hat{p}_e)^n=\hat{p}_e$] that in the flavor basis has the components $(\hat{p}_e)_{\alpha\beta}=\delta_{\alpha e}\delta_{\beta e}$ and a second adimensional quantity

$$z=VL. \tag{A11}$$

Writing the S matrix in an expanded form, squaring the element $S_{\beta\alpha}$, and collecting all terms proportional to (y^nz^m) one can obtain the transition probability as a power series in both y and z:

$$P_{\alpha\to\beta}(L,E_\nu)=P_{\alpha\to\beta}(y,z)=\sum_{n=2}^{\infty}\sum_{m=0}^{\infty}c_{n,m}^{\alpha\to\beta}y^nz^m. \tag{A12}$$

Naively one could expect to see terms of order (y^0z^2), (yz), and (yz^2) but they are present only on the diagonal of the S matrix and are irrelevant for the transition probabilities.

Note that the set of coefficients $c_{n,0}^{\alpha\to\beta}$ are of course identical to the vacuum expansion. From this we can deduce the very important fact: if z is small, that is, when the ν path length is much shorter than the matter length V^{-1}, the oscillation probabilities are approximately equal to the vacuum case. This in a sense is not an entirely obvious fact, because a condition on the path length does not say anything about the importance of the matter effects on the neutrino masses and mixing. It is indeed possible that E_ν and V are such that the mixing parameters are entirely different from the vacuum case (for example, one could sit on a MSW resonance), however, if $L\ll V^{-1}$, the oscillation probabilities will coincide with the vacuum case. This result, especially in the 3ν case, appear as the consequence of some remarkable ''cancellations'' between the effective values of the mixing parameters and squared masses, however, in this formalism it is entirely natural and obvious.

Some important symmetry of the coefficients are the following:

$$\begin{aligned}
&c_{n,m}^{\alpha\to\beta}=+c_{n,m}^{\beta\to\alpha}=+c_{n,m}^{\bar{\alpha}\to\bar{\beta}}=+c_{n,m}^{\bar{\beta}\to\bar{\alpha}}\\
&\text{for } n \text{ even and } m \text{ even},\\
&c_{n,m}^{\alpha\to\beta}=+c_{n,m}^{\beta\to\alpha}=-c_{n,m}^{\bar{\alpha}\to\bar{\beta}}=-c_{n,m}^{\bar{\beta}\to\bar{\alpha}}\\
&\text{for } n \text{ even and } m \text{ odd},\\
&c_{n,m}^{\alpha\to\beta}=-c_{n,m}^{\beta\to\alpha}=-c_{n,m}^{\bar{\alpha}\to\bar{\beta}}=+c_{n,m}^{\bar{\beta}\to\bar{\alpha}}\\
&\text{for } n \text{ odd and } m \text{ even},\\
&c_{n,m}^{\alpha\to\beta}=-c_{n,m}^{\beta\to\alpha}=+c_{n,m}^{\bar{\alpha}\to\bar{\beta}}=-c_{n,m}^{\bar{\beta}\to\bar{\alpha}}\\
&\text{for } n \text{ odd and } m \text{ odd}.
\end{aligned} \tag{A13}$$

Note how the matter effects when they enter with an odd power of the potential have opposite signs for ν and $\bar{\nu}$.

An explicit calculation of the coefficients of lower order in y gives for $n=2$

$$c_{2,m(\mathrm{odd})}^{\alpha\to\beta}=0 \tag{A14}$$

while for m even one has

$$c_{2,m(\mathrm{even})}^{\alpha\to\beta}=[\hat{h}_{\alpha\beta}\hat{t}_{\alpha\beta}^*]d_{2,m}, \tag{A15}$$

where $d_{2,m}$ are simple numerical coefficients:

$$d_{2,m(\mathrm{even})} = i^m \sum_{k=0}^{m} \frac{(-1)^k}{(k+1)!(m+1-k)!} = \frac{2}{(m+2)!} i^m. \tag{A16}$$

For the elements with $n=3$ one has

$$c^{\alpha\to\beta}_{3,m(\mathrm{even})} = \mathrm{Im}[\hat{h}^*_{\alpha\beta}(\hat{h}^2)_{\alpha\beta}] d_{3,m}, \tag{A17}$$

$$c^{\alpha\to\beta}_{3,m(\mathrm{odd})} = \frac{1}{6}\mathrm{Re}\{\hat{h}^*_{\alpha\beta}[2\hat{h}_{\alpha e}\hat{h}_{e\beta} - (\hat{h}^2)_{\alpha\beta}(\delta_{\alpha e}+\delta_{\beta e})]\} d_{3,m}, \tag{A18}$$

where the quantities $d_{3,m}$ are numerical coefficients:

$$d_{3,m(\mathrm{even})} = 2i^m \sum_{k=0}^{m} \frac{(-1)^k}{(k+1)!(m+2-k)!} = \frac{2}{(m+2)!} i^m \quad \text{for } m \text{ even}, \tag{A19}$$

$$d_{3,m} = 12 i^{m-1} \sum_{k=0}^{m} \frac{(-1)^k}{(k+1)!(m+2-k)!} = \frac{12(m+1)}{(m+3)!} i^{m-1} \quad \text{for } m \text{ odd} \tag{A20}$$

(the coefficients have been defined so that $d_{2,0}=d_{3,0}=d_{3,1}=1$).

It is useful, for example, when considering an experiment with a fixed baseline, to resum over all z terms, and express the probability again as a power series in y (that corresponds then to a power series in E_ν^{-1}), with coefficients that are distance dependent. For the lowest terms the sum is easily obtained:

$$\sum_{m=0}^{\infty} d_{2,m} z^m = \sum_{m(\mathrm{even})=0}^{\infty} d_{2,m} z^m = \left(\frac{2}{z}\right)^2 \sin^2\left(\frac{z}{2}\right), \tag{A21}$$

$$\sum_{m(\mathrm{odd})=1}^{\infty} d_{2,m} z^m = \frac{48}{z^3}\left[\sin^2\left(\frac{z}{2}\right) - \frac{z}{4}\sin(z)\right]. \tag{A22}$$

The reason to keep separate the sums of the m-even and m-odd contributions is because they have different symmetry properties under a CP transformation. For m even (odd) the $c^{\alpha\to\beta}_{n,m}$ coefficients have the same (opposite) sign for ν's and $\bar{\nu}$'s.

It can be interesting to verify the results derived above in the special case of two neutrino mixing, when simple exact expressions for oscillations probabilities exist. This is done in the next section.

APPENDIX B: TWO FLAVOR MIXING CASE

It can be useful to to discuss $\nu_e \leftrightarrow \nu_\mu$ or $\nu_e \leftrightarrow \nu_\tau$ oscillations in the case of two flavor oscillations when the explicit calculation of the oscillation probabilities in matter is very simple. Moreover, this case is an exact solution in two interesting limiting cases: (1) The limit $x_{12}\to 0$ (Δm^2_{12} small). In this case one has to replace $\theta\to\theta_{13}$, $\Delta m^2 \to \Delta m^2_{23}$. The oscillation probabilities for the $\nu_e \leftrightarrow \nu_\mu$ and $\nu_e \leftrightarrow \nu_\tau$ transitions are then given by the two flavor formula multiplying by $\sin^2\theta_{23}$ and $\cos^2\theta_{23}$; (2) the limit $\theta_{13}\to 0$. In this case one has to make the replacements $\theta\to\theta_{12}$, $\Delta m^2 \to \Delta m^2_{12}$. The oscillation probabilities for the $\nu_e \leftrightarrow \nu_\mu$ and $\nu_e \leftrightarrow \nu_\tau$ transitions are then given by the two flavor formula multiplying by $\cos^2\theta_{23}$ and $\sin^2\theta_{23}$.

In the two flavor approximation the vacuum oscillation probability is

$$P_{\mathrm{vac}}(\nu_e \to \nu_\mu) = \sin^2 2\theta \sin^2\left[\frac{\Delta m^2 L}{4E_\nu}\right]. \tag{B1}$$

To have the oscillations in matter we simply have to perform the replacements $\theta\to\theta_{\mathrm{m}}$ and $\Delta m^2 \to (\Delta m^2)_{\mathrm{m}}$ with

$$\sin^2 2\theta_{\mathrm{m}} = \sin^2 2\theta \left[\sin^2 2\theta + \left(\cos 2\theta \mp \frac{2E_\nu V}{\Delta m^2_{23}}\right)^2\right]^{-1} \tag{B2}$$

and

$$(\Delta m^2)_{\mathrm{m}} = \Delta m^2 \sqrt{\sin^2 2\theta + \left(\cos 2\theta \mp \frac{2E_\nu V}{\Delta m^2}\right)^2}. \tag{B3}$$

The minus (plus) sign refers to neutrinos (antineutrinos). It can be seen that in general: (i) the oscillation probabilities in vacuum and in matter can be very different from each other; (ii) the oscillation probabilities in matter for ν and $\bar{\nu}$'s are also in general very different.

We are interested in the probability for large E_ν. For vacuum oscillations it is straightforward to expand the probability as a power series in $y = \Delta m^2 L/(4E_\nu)$:

$$P_{\mathrm{vac}} \simeq \sin^2 2\theta \left(\frac{\Delta m^2 L}{4E_\nu}\right)^2 - \frac{\sin^2 2\theta}{3}\left(\frac{\Delta m^2 L}{4E_\nu}\right)^4 + \ldots. \tag{B4}$$

To compute the same expansion for the probabilities in matter it is useful to introduce the variable

$$\varepsilon = \frac{\Delta m^2}{2VE_\nu}; \tag{B5}$$

using the shortened notation $s=\sin 2\theta$, $c=\cos 2\theta$, the oscillation probability in matter can then be rewritten as

$$P_{\mathrm{mat}}(\nu_e \to \nu_\mu) = \frac{s^2\varepsilon^2}{1 \mp 2c\varepsilon + \varepsilon^2} \sin^2\left[\frac{VL}{2}\sqrt{1 \mp 2c\varepsilon + \varepsilon^2}\right]. \tag{B6}$$

Developing in a power series in ε and writing for simplicity $\alpha = VL/2$ one obtains

$$P_{\mathrm{mat}}(\nu_e \to \nu_\mu) = s^2\varepsilon^2 \sin^2\alpha \pm 2s^2 c\varepsilon^3(\sin^2\alpha - \alpha \sin\alpha\cos\alpha) + O(\varepsilon^4) \tag{B7}$$

that can be rewritten as

$$P_{\rm mat}(\nu_e\to\nu_\mu)=\sin^2 2\theta\left(\frac{\Delta m^2 L}{4E_\nu}\right)^2\left[\frac{1}{\alpha^2}\sin^2\alpha\right]+\frac{\sin^2 2\theta\cos 2\theta}{3}\left(\frac{\Delta m^2 L}{4E_\nu}\right)^3\left[\left(\frac{6}{\alpha^3}\right)\times(\sin^2\alpha-\alpha\sin\alpha\cos\alpha)\right]+\cdots. \quad \text{(B8)}$$

We can note that the first (second) term is symmetric (antisymmetric) for the replacement $V\to -V$ that is replacing ν with $\overline{\nu}$.

Developing the expression (B8) for small α (that is for $L<V^{-1}$) and reinserting the definition one obtains

$$P_{\rm mat}(\nu_e\to\nu_\mu)=\sin^2 2\theta\left(\frac{\Delta m^2 L}{4E_\nu}\right)^2\left[1-\frac{(VL)^2}{12}+\cdots\right]+\frac{\sin^2 2\theta\cos 2\theta}{3}\left(\frac{\Delta m^2 L}{4E_\nu}\right)^3\times VL\left[1-\frac{(VL)^2}{15}+\cdots\right]+\cdots. \quad \text{(B9)}$$

We have obtained with an explicit calculation a set of interesting results for the oscillation probability in the limit of large energy: (i) The oscillation probabilities for ν's and $\overline{\nu}$'s become asymptotically equal, and vanish with a leading contribution of order $y^2\sim E_\nu^{-2}$; (ii) the matter effects generate a correction of opposite sign for ν's and $\overline{\nu}$'s. This correction vanishes more rapidly with increasing energy $\propto y^3\sim E_\nu^{-3}$; (iii) for small path length $L\lesssim V^{-1}$ the matter effects grow linearly with the matter potential V; (iv) again for small path length the leading-order term of the oscillation probability grows with the path length $\propto L^2$, while the correction due to the matter effects grows more rapidly $\propto L^4$.

Comparing Eqs. (B8) and (B9) with Eqs. (32) and (39) one can see that we have reproduced with an explicit calculation the results for the leading-order term of the oscillation probability and for the matter effects. It is also easy to see that in the two flavor case considered here the free Hamiltonian and its square can be written in the flavor basis as

$$\mathcal{H}_0=\frac{\Delta m^2}{4E_\nu}\begin{bmatrix}-\cos 2\theta & \sin 2\theta\\ \sin 2\theta & \cos 2\theta\end{bmatrix},\quad (\mathcal{H}_0)^2=\left(\frac{\Delta m^2}{4E_\nu}\right)^2\begin{bmatrix}1 & 0\\ 0 & 1\end{bmatrix}. \quad \text{(B10)}$$

Calculating the coefficients $A_{e\mu}$, $B_{e\mu}$, and $C_{e\mu}$ according to the general formulas (36), (37), and (38) one obtains $A=\sin^2 2\theta$, $B=0$ (CP and T violation effects vanish in the two flavor case), and $C=\cos 2\theta\sin^2 2\theta/3$ in agreement with the general result.

APPENDIX C: MASSES AND MIXING FOR LARGE MATTER EFFECTS

The dependence of the effective squared mass differences and mixing parameters in matter on the product ρE_ν is shown in Figs. 5, 6, and 7 (in the figures we assumed an electron fraction of $\frac{1}{2}$, therefore the density ρ and the potential V are simply proportional). Several important features are clearly visible.

(1) The squared mass eigenvalues and of the mixing parameters in matter are in general very different for neutrinos and antineutrinos. Reversing the sign of Δm^2_{23}, the behavior of ν and $\overline{\nu}$'s to a good approximation is simply exchanged.

(2) All four mixing parameters (the tree angles and the phase) change when matter is present, however, when the two mass scales Δm^2_{12} and $|\Delta m^2_{23}|$ are of different orders of magnitude, as indicated by the the data, the angle θ_{23} and the phase δ remain approximately constant while the angles θ_{12} and θ_{13} change much more dramatically.

(3) We can recognize several ranges of the parameter $a=2E_\nu V$ where the behavior of the solution has different characteristics.

(i) When $2E_\nu V\ll\Delta m^2_{12}$, all matter effects are negligible and the oscillations develop as in the vacuum case.

(ii) For $2E_\nu V\ll|\Delta m^2_{23}|$ the effective mass and mixing of the state ν_3 remain unchanged, but Δm^2_{12} and θ_{12} can be modified by matter effects (this is interesting only if $\Delta m^2_{12}\ll|\Delta m^2_{23}|$). In this situation it is a good approximation to use the well-known two flavor formulas to obtain $(\Delta m^2_{12})^{\rm m}$ and $\theta^{\rm m}_{12}$ as a function of $2VE_\nu$.

(iii) When $2E_\nu V\simeq|\Delta m^2_{23}|$ there is a resonance ($\theta^{\rm m}_{13}$ becomes $\pi/4$). The resonance is present for neutrinos if Δm^2_{23} positive or for antineutrinos if Δm^2_{23} is negative.

(iv) When $2VE_\mu\gg|\Delta m^2_{23}|$, the behavior of the mixing angles and squared mass eigenvalues takes a simple form that will be discussed below.

In the study of the effective parameters for large matter effects $[|\Delta m^2_{23}|/(2VE_\nu)\to 0]$ one has to distinguish two cases.

Case A corresponds to neutrinos for Δm^2_{23} positive or to antineutrinos for Δm^2_{23} negative. In this case one has

$$(\Delta m^2_{12})^{\rm m}\to\Delta m^2_{23},$$

$$(\Delta m^2_{23})^{\rm m}\to 2VE_\nu,$$

$$\sin^2\theta^{\rm m}_{13}\to 1,\quad \cos^2\theta^{\rm m}_{13}\to\sin^2\theta_{13}\left(\frac{\Delta m^2_{23}}{2E_\nu V}\right)^2,$$

$$\sin^2\theta^{\rm m}_{12}\to\sim 1,\quad \cos^2\theta^{\rm m}_{12}\to{\rm const}\simeq\sin^2\theta_{12}\frac{\Delta m^2_{12}}{\Delta m^2_{23}}.$$

This means that $|\nu^{\rm m}_3\rangle$ becomes asymptotically a massive pure $|\nu_e\rangle$ state, therefore $\theta_{13}\to\pi/2$ and $\cos^2\theta_{13}$ vanishes rapidly $(\propto 2E_\nu V)^{-2}$. The angle θ_{12} tends to a constant value, reflecting the fact that the ν_e flavor is ''sucked away'' at the same rate from the $|\nu_1\rangle$ and $|\nu_2\rangle$ states. The squared mass

difference $(\Delta m^2_{23})^{\rm m}$ grows without bound ($\to 2E_\nu V$), while $(\Delta m^2_{12})^{\rm m}$ approaches the constant value ($\to \Delta m^2_{23}$).

Case B corresponds to neutrinos for Δm^2_{23} negative or to antineutrinos for Δm^2_{23} positive. In this case one has

$$(\Delta m^2_{12})^{\rm m} \to 2VE_\nu ,$$

$$(\Delta m^2_{23})^{\rm m} \to \Delta m^2_{23} ,$$

$$\sin^2\theta^{\rm m}_{13} \to \sin^2\theta_{13}\left(\frac{\Delta m^2_{23}}{2E_\nu V}\right)^2 , \quad \cos^2\theta^{\rm m}_{13} \to 1,$$

$$\sin^2\theta^{\rm m}_{12} \to \sin^2\theta_{12}\left(\frac{\Delta m^2_{12}}{2E_\nu V}\right)^2 , \quad \cos^2\theta^{\rm m}_{12} \to 1.$$

In this case it is $|\nu^{\rm m}_1\rangle$ that becomes the massive pure $|\nu_e\rangle$ state, therefore both θ_{12} and θ_{13} asymptotically vanish $\propto (2E_\nu V)^{-1}$, and it is $(\Delta m^2_{12})^{\rm m}$ that grows large ($\to 2E_\nu V$) while Δm^2_{23} remains approximately unchanged. In both cases the modifications to the angle θ_{23} and the phase δ are small and vanish for $\Delta m^2_{12}/|\Delta m^2_{23}|$ small.

Note that the behavior of the effective masses and mixing parameters is strikingly different for ν's and $\bar{\nu}$'s. However, there are some important cancellations. For example, collecting the expressions for the different factors one can verify that the the effective Jarlskog parameter in matter [$J_{\rm m} = (c^{\rm m}_{13})^2 s^{\rm m}_{13} s^{\rm m}_{12} c^{\rm m}_{12} s^{\rm m}_{23} c^{\rm m}_{23} \sin\delta_{\rm m}$] is equal for ν and $\bar{\nu}$:

$$J^\nu_{\rm m} = J^{\bar{\nu}}_{\rm m} \to J_{\rm vacuum} \frac{\Delta m^2_{13}\Delta m^2_{12}}{(2E_\nu V)^2} \tag{C1}$$

(see Fig. 7 for the numerical calculation), as it is the case for the product of the three effective squared mass differences:

$$(\Delta m^2_{12})^\nu_{\rm m}(\Delta m^2_{23})^\nu_{\rm m}(\Delta m^2_{13})^\nu_{\rm m} = (\Delta m^2_{12})^{\bar{\nu}}_{\rm m}(\Delta m^2_{23})^{\bar{\nu}}_{\rm m}(\Delta m^2_{13})^{\bar{\nu}}_{\rm m} \to \Delta m^2_{23}(2VE_\nu)^2. \tag{C2}$$

Combining the two results satisfies Eq. (45).

[1] Super-Kamiokande Collaboration, Y. Fukuda *et al.*, Phys. Rev. Lett. **81**, 1562 (1998); Soudan 2 Collaboration, Phys. Lett. B **449**, 137 (1999); MACRO Collaboration, *ibid.* **434**, 451 (1998); M. Ambrosio *et al.*, hep-ex/0001044.

[2] Homestake Collaboration, K. Lande *et al.*, Astrophys. J. **496**, 505 (1998); SAGE Collaboration, J. N. Abdurashitov *et al.*, Phys. Rev. C **60**, 055801 (1999); GALLEX Collaboration, W. Hampel *et al.*, Phys. Lett. B **447**, 127 (1999); Kamiokande Collaboration, Y. Fukuda *et al.*, Phys. Rev. Lett. **77**, 1683 (1996); Super-Kamiokande Collaboration, Y. Fukuda *et al.*, *ibid.* **81**, 1158 (1998); **81**, 4279 (1998); **82**, 2430 (1999); **82**, 1810 (1999).

[3] Chooz Collaboration, M. Apollonio *et al.*, Phys. Lett. B **420**, 397 (1998); **466**, 415 (1999); Palo Verde Collaboration, F. Boehm *et al.*, Phys. Rev. D **62**, 072002 (2000).

[4] LSND Collaboration, C. Athanassopoulos *et al.*, Phys. Rev. C **54**, 2685 (1996); **58**, 2489 (1998).

[5] N. Cabibbo, Phys. Lett. **72B**, 33 (1978); V. Barger, K. Wisnant, and R. J. N. Phillips, Phys. Rev. Lett. **45**, 2084 (1980).

[6] J. Arafune and J. Sato, Phys. Rev. D **55**, 1653 (1997); J. Arafune, M. Koike, and J. Sato, *ibid.* **56**, 3093 (1997); **60**, 119905(E) (1999); M. Tanimoto, Phys. Lett. B **345**, 373 (1998); H. Minakata and H. Nunokawa, *ibid.* **413**, 369 (1997); Phys. Rev. D **57**, 4403 (1998).

[7] A. Donini, M. B. Gavela, P. Hernández, and S. Rigolin, Nucl. Phys. **B574**, 23 (2000); M. Tanimoto, Phys. Rev. D **55**, 322 (1997); Prog. Theor. Phys. **97**, 901 (1997); S. M. Bilenky, C. Giunti, and W. Grimus, Phys. Rev. D **58**, 033001 (1998); A. De Rujula, M. B. Gavela, and P. Hernandez, Nucl. Phys. **B547**, 21 (1999); K. Dick *et al.*, *ibid.* **B562**, 29 (1999).

[8] S. Geer, Phys. Rev. D **57**, 6989 (1998); **59**, 039903(E) (1999); A. de Rújula, M. B. Gavela, and P. Hernández, Nucl. Phys. **B547**, 21 (1999).

[9] For a review, see C. Albright *et al.*, hep-ex/0008064. Information on high-energy neutrino factory studies can be found at http://www.cap.bnl.gov/mumu/, http://www.fnal.gov/projects/muon_collider/, and http://muonstoragerings.web.cern.ch/muonstoragerings/

[10] Masafumi Koike and Joe Sato, Phys. Rev. D **61**, 073012 (2000); **62**, 079903(E) (2000).

[11] Hisakazu Minakata and Hiroshi Nunokawa, Phys. Lett. B **495**, 369 (2000).

[12] J. Sato, hep-ph/0008056; M. Koike, T. Ota, and J. Sato, hep-ph/0011387.

[13] Y. Kuno, in Proceedings of the Workshop on High Intensity Secondary Beam with Phase Rotation, Institute for Chemical Research, Kyoto University, Japan, 1998.

[14] It should be noted that the study of *T* violation, because of the structure of the Earth's crust could require two experiments with two accelerators (located at points A and B) and two detectors (located at points B and A) to insure that also the matter potential $V(t)$ that the neutrinos encounter during their path is replaced by the *T*-transformed one. This point has been made by H. Nunokawa and O. Yasuda (private communication).

[15] A. Cervera *et al.*, Nucl. Phys. **B579**, 17 (2000).

[16] A. Bueno, M. Campanelli, and A. Rubbia, Nucl. Phys. **B589**, 577 (2000).

[17] Particle Data Book, D. Groom *et al.*, Eur. Phys. J. C **15**, 1 (2000).

[18] A. Smirnov, in Proceedings of Neutrino 2000.

[19] G. L. Fogli *et al.*, Phys. Rev. D **62**, 013002 (2000); **59**, 033001 (1999).

[20] The parametrization (7) of the mixing matrix, suggested originally to describe the mixing in the quark sector, turned out to be very well suited for neutrinos, since solar ν experiments

essentially measure Δm^2_{12} and the mass components of $|\nu_e\rangle$, while atmospheric and reactor experiments measure Δm^2_{23} and the flavor components of $|\nu_3\rangle$. In the chosen parametrization this corresponds to the row and column of the mixing matrix with the simplest form, since the phase does not enter into the expression for the module of any element.

[21] L. Wolfenstein, Phys. Rev. D **17**, 2369 (1978); **20**, 2634 (1979); S. P. Mikheyev and A. Yu. Smirnov, Yad. Fiz. **42**, 1441 (1985) [Sov. J. Nucl. Phys. **42**, 913 (1985)].

[22] H. W. Zaglauer and K. H. Schwarzer, Z. Phys. C **40**, 273 (1988).

[23] C. Jarlskog, Phys. Rev. Lett. **55**, 1039 (1985).

[24] P. F. Harrison, D. H. Perkins, and W. G. Scott, Phys. Lett. B **458**, 79 (1999).

[25] Paolo Lipari, Phys. Rev. D **61**, 113004 (2000).

[26] Osamu Yasuda (private communication).

[27] This is of course an optimistic view of the present situation, since it accepts as valid interpretations that are still questioned, and a conservative view because it ignores the LSND results.

[28] Burton Richter, hep-ph/0008222.

[29] V. Barger, S. Geer, R. Raja, and K. Whisnant, Phys. Rev. D **63**, 113011 (2001).